10-1-2018 2:00 PM

An Integrated Approach to Analyzing Arteriolar Network Hemodynamics.

Zahra Farid
The University of Western Ontario

Supervisor
Jackson, Dwayne N.
The University of Western Ontario Joint Supervisor
Goldman, Daniel
The University of Western Ontario

Graduate Program in Medical Biophysics
A thesis submitted in partial fulfillment of the requirements for the degree in Master of Science

Abstract

The objective of this thesis was to optimize our technique for studying blood flow in arteriolar networks by including capillary resistance and venular network geometry. We aimed to validate our technique using experimental flow measurements and Murray's law. First, arteriolar and venular networks were reconstructed from intravital videomicroscopy (IVVM) images of the gluteus maximus muscle, and capillary resistance was estimated and distributed to each terminal arteriole (TA) segment according to its diameter. Resistance for small arterioles and venules that were likely missed in our IVVM experiments were also added to each TA segment in our reconstructed networks based on measured branching properties of arteriolar and venular networks. We acquired fluorescent streaks for flow measurements in an arteriolar network, which validated flow simulations from our steady state, two-phase model. We found a strong match between measured arteriolar blood flow and predicted arteriolar flows using capillary resistance, venular geometry, and small-vessel resistance. Experimental data gave a Murray's law exponent of 2.9, to which we compared predicted values from blood flow simulations. Using n=8 networks, we found a Murray's law exponent of 2.78. Our results show that our network-oriented approach is moving towards more accurately predicting hemodynamic properties of arteriolar networks under baseline conditions.

Keywords

Blood flow, Skeletal muscle, Arterioles, Arteriolar network, Venules, Microcirculation, Network analysis, Intravital videomicroscopy, Mathematical modeling, Murray's law.

List of Abbreviations and Symbols

RBC: red blood cell

WBC: white blood cell

GM: gluteus maximus

HCT: hematocrit

IVVM: intravital video-microscopy

MTT: mean transit times

NPY: neuropeptide Y

SNS: sympathetic nervous system

NE: norepinephrine

ATP: adenosine triphosphate

NO: nitric oxide

COX: cyclooxygenase

EDHF: endothelial derived hyperpolarizing factor

5'NUC: 5'-nucleotidase

V_{mean}: mean red blood cell flow velocity

A_{vessel}: vessel cross-sectional area

V_{centre}: centerline velocity

V_{RBC}: red blood cell velocity

V_{ratio}: velocity ratio

CFL: red blood cell-free layer

V_{wall}: velocity at wall

WSR: wall shear rate

V_{max}: maximum velocity

H_T: tube hematocrit

H_D: discharge hematocrit

Q: blood flow

ΔP: pressure drop

η: viscosity

r: vessel radius

L: vessel length

$\Re$: resistance

R_D: diameter ratio

R_L: length ratio

R_B: bifurcation ratio

S/E: segment-to-element ratio

CV: coefficient of variation

TA: terminal arterioles

Co-Authorship Statement

Zahra Farid performed all simulations and analyses in Chapter 2. Experimental images used in the analyses were obtained from previously acquired data by Mohammed Al Tarhuni, and newly acquired data by Kent Lemaster. Dr. Dwayne Jackson and Dr. Daniel Goldman formulated and guided the conception and design of the experiments and analyses. Dr. Dwayne Jackson provided physiological input and interpretation on results, while Dr. Daniel Goldman provided theoretical/mathematical input and interpretation. The experimental tools were developed and provided by Dr. Dwayne Jackson. The mathematical tools were developed and provided by Dr. Daniel Goldman, with some developments and modifications by Zahra Farid.

Acknowledgments

I want to begin by thanking God for this opportunity to complete my thesis, and for every other blessing in my life! My success is only by Allah.

To my supervisors, Dr. Dwayne Jackson and Dr. Daniel Goldman, thank you for giving me the most valuable Master's experience! I am so grateful for your unwavering guidance and mentorship, and for your presence, attention, and feedback every meeting. I am eternally grateful for the scientific and personal growth I have experienced in these short two years. Thank you for setting me up to be successful! Thank you, Dan, for your patience and support while I learned and applied your mathematical models. Thank you for your sharing your knowledge and expertise with me, and for always being so understanding and kind. Your gentle demeanor is a quality that every student would wish for in a mentor! Thank you, Dwayne, for being not only my mentor, but also my friend. Thank you for all your wisdom and motivation. I have learned more than just microvascular physiology from our discussions; I have learnt what it means to be resilient, successful, and extraordinary! I have watched you lead and influence, not only me, but also thousands of people with your incredible positivity and passion for health! You are a walking miracle of God, and I am so blessed to know you!

To the staff at Medical Biophysics, thank you for working so hard to help us meet deadlines, and for organizing successful events in the department!

To my family, thank you for taking such good care of me while I focus on my program! Thank you for raising me with values that have helped me persevere and overcome every challenge in my life! I attribute my patience and strength to you!

To my best friends, thank you for being the most genuine and caring sisters! Thank you for your efforts to help me maintain my physical, emotional, and mental health every day! I appreciate your love and friendship, and all your emotional and social support!

Last, but not the least, to my love, Eyad, thank you for making these last few years the happiest years of my life! Thank you for being a constant source of love, happiness, and tranquility in my life! Thank you for believing in me (and in us) and for supporting every dream of mine! Thank you for being so patient, kind and understanding! Most importantly, thank you for introducing me to One Piece. You have been the greatest blessing from above.

Table of Contents

List of Tables

List of Figures

List of Appendices

Chapter 1

Introduction to Network Analysis

1.1 Introduction

In this chapter, we present a historical review on seminal studies that have contributed to network-oriented analysis, focusing on the development of tools from experimental to theoretical methods. Through this review, we aim to both highlight the history of network analysis and demonstrate why it is an ideal approach in microvascular research. At the end of the chapter, we highlight studies from own lab that have overcome challenges in microvascular research and that have led us to our current thesis (*Chapter 2*).

1.2 Beginning of an Era: Experimental Contributions

The microcirculation has been notably reviewed in recent years by several prominent microvascular researchers, such as Mary P. Weideman in *An Introduction to the Microcirculation* [54] and Paul C. Johnson in the 2008 Volume of *The Handbook of Physiology* [29], whose seminal overviews we reference heavily in our own review of network analysis in the microcirculation. Our historical introduction begins in 1628, before the development of microscopes, when the existence of vessels "too small to be seen with the naked eye" was first hypothesized by William Harvey [29]. Harvey postulated that the path for blood flow in tissues must consist of channels or pores that connect arteries and veins, based on his argument that blood ejected from the heart must circulate back [19,22].

It was not until after the development of the single-lens microscope that Harvey's postulations were validated with experimental observations. The first simple single-lens microscope was developed by Anton van Leeuwenhoek in the seventeenth century (1632-1723) and marks one of the most significant events in the history of experimental biology. Leeuwenhoek's work in the study of microscopy set the stage for future biologists, including Marcello Malpighi, who was the first person to confirm Harvey's postulation with his detailed observations of the microcirculation in the tortoise lung in 1661 [29]. Malpighi used a simple single-lens microscope to study and describe the

structure of a living lung tissue and its microvasculature. Following these scientific observations, Leeuwenhoek used his microscopes to describe blood flow in tadpoles. Leeuwenhoek observed, and classified arteries and veins based on the direction of blood flow, noting the close similarity in structure [26]. To best distinguish between these vessels *in vivo*, vessels that carry blood to terminal vessels are arteries, and vessels that carry blood back to the heart are veins [54].

Further advancements in microscopy techniques made it possible to observe the circulation in other animal models. As an example, shortly after the rise of the microscope, John Marshall designed a microscope for observing blood circulation in living fish [10]. Part of the microscope design was a built-in coffin that functioned to restrain the fish. Following blood flow, major observations made by Stephen Hales (1700s) on changes in vessel diameter (vessel contraction) led to the concept of blood flow resistance and therefore, regulation. Hales was also the first to directly measure blood pressure by connecting a glass tube to a cannulated carotid artery of various animals [54]. Up until 1838, most structural information on the microvasculature was based on qualitative descriptions. Johannes Muller changed this by being the first to measure capillary diameters in various animal tissues [54]. Muller also correctly postulated the function of capillaries by describing them as porous vessels through which fluid can escape.

1.3 Advancements Through the Study of Capillaries

The studies of capillaries and their role in the microcirculation were continued by many others, and later highlighted by Nobel Prize winner August Krogh in his comprehensive account of The Anatomy and Physiology of Capillaries [31]. Krogh believed that the ultimate function of the microcirculation relied on the capillaries as exchange vessels, and his work served to answer the question on the mechanism and control of oxygen supply to muscle fibers [31]. Krogh explained the mechanism as a function of the distribution and number of capillaries in a tissue, while the control as a function of the

contractility of the capillary vessels. The latter concept caused a controversy and was subsequently dispelled by other research.

Over a decade later, Benjamin William Zweifach made his own contributions to the study of capillary structure and function. In 1937 and 1939, Zweifach used a micromanipulative technique to look at permeability of living capillaries in various tissues, such as the mesentery, tongue and skin, of the frog [56]. From his observations, two types of capillary vessels were described and distinguished based on whether they were partially or completely free of smooth muscle cells, and named arteriolo-venular bridge and true capillaries, respectively [55]. Figure 1 shows the blood outline of the vessels of the frog. Their functions were described in terms of structural distribution, size, and pattern of blood flow.

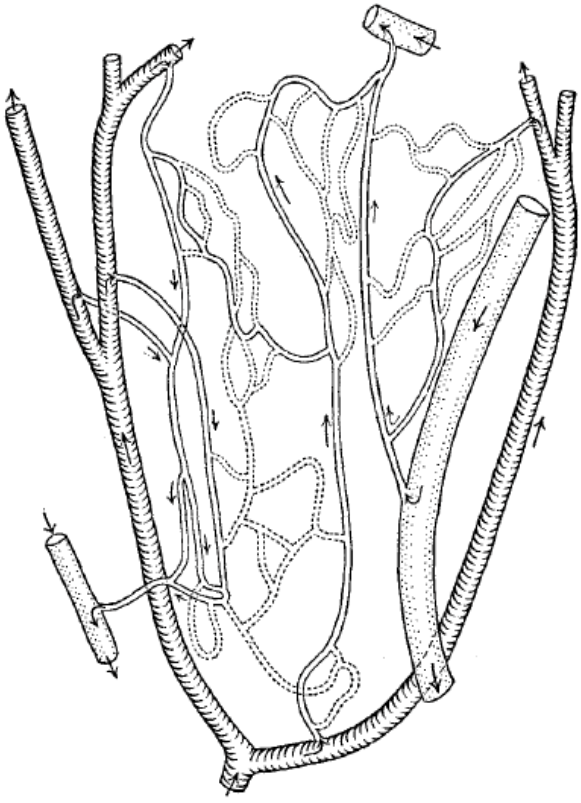

Figure 1: Camera lucida outline of vascular pattern of small blood vessels in nictitating membrane of the frog. Arterioles are cross lined, venules stippled, a-v

bridges have solid outlines, true capillaries have broken outlines. Note the bridge between the two larger venules. [Reference 55: Zweifach BW. The structure and reactions of the small blood vessels in amphibia. *American Journal of Anatomy* **60**: 473-514, 1937].

The study of capillaries also revealed the most interesting behaviors of the microcirculation, the Fahraeus and Fahraeus-Lindqvist effects, which set it apart from that in the macrocirculation. In 1929, Fahraeus found that in small glass tubes (<200 μm in diameter), the measured tube hematocrit decreased as the tube diameter decreased [17]. After cutting flow through the glass tube, the tube hematocrit, or the fraction of red blood cells in the tube, was obtained by spinning blood from the tube in a centrifuge and separating the red blood cells from the plasma. A few years later in 1931, Fahraeus and Lindqvist reported measurements of viscosity (μ) in small tubes and found that viscosity also decreased with tube diameter [18]. By measuring fluid flow rate Q, pressure head ΔP, and the dimensions of the tube (length L and radius r), viscosity of the fluid can be calculated using the Poiseuille law:

$Q = \frac{\pi \cdot \Delta P \cdot r^4}{8 \cdot L \cdot \mu}$, to give $\mu = \frac{\pi \cdot \Delta P \cdot r^4}{8 \cdot L \cdot Q}$

1.4 Development of Classification Systems

One of the most important tools in microvascular network analysis is the ability to classify vessels in a network and use this classification to compare the structure and function between networks. Two different classification techniques were developed around this time: the Horton-Strahler method known as centripetal, which assigns 1st order to the terminal vessels and 2nd order to a vessel connecting two 1st order vessels [48]. This method is useful for vessels close to the capillary level, but becomes less useful at levels farther upstream. The second classification scheme developed by Mary P. Weideman, known as the centrifugal scheme, assigns 1st order to the largest arteriole and 2nd order to the next successive branch vessel [53]. The successive branches are based on a determined size and branch angle, which are assessed by the researcher, and therefore can be subjective in nature. If designations between researchers are consistent, comparisons between networks are made useful and accurate.

Before the application of these ordering schemes, topological levels would be identified using vessel diameter alone. This simple approach was useful for many *in vivo* hemodynamic studies, such as that by Lipowsky and Zweifach [36], who were some of the original advocates of the network-oriented approach. In their study, Lipowsky and Zweifach compared distributions of computed intravascular pressure, pressure gradients, and wall shear stress to measured values in arteriolar and venular vessels with diameters ranging up to 46 μm in the cat mesentery. The distributions of intravascular pressures are shown in Figure 2. Their computations were based on a network approach using a Poiseuille flow model, where flow parameters across all vessels in the network are considered in the computation. The comparisons they made demonstrated the value of network analysis and the need for continued work in developing network hemodynamic models.

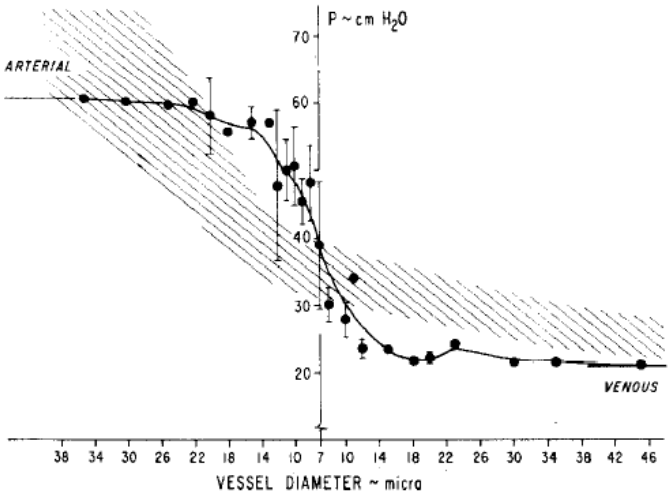

Figure 2: Distribution of mean intravascular pressure. Horizontal lines to the left and right of the ordinate represent the assumed boundary pressures at the boundary nodes. Computed mean intravascular pressures, averaged at each discrete diameter are represented by the circular symbols bracketed by a band of ± 1σ (where σ equals the standard deviation). Standard deviations less than 1 cm H_20 are not shown. The solid line represents a cubic spline fit fairing of the computed pressures. The cross-hatched area represents the band of intravascular pressures measured *in vivo* for 150 modules. [Reference 36: Lipowsky HH, and Zweifach, B.W. Network analysis of microcirculation of cat mesentery. *Microvascular Research* **7**: 73-83, 1974].

Prior to the quantification of functional parameters in the cat mesentery, Frasher and Wayland conducted a detailed analysis of the repeating modular organization of the cat mesenteric microcirculation in 1972. A major goal in their research was to understand the structural-functional relationship in this microvascular bed [20]. They present two functional categories, nutritional and operant, which define the structural-functional relationship. In the nutritional category, flow is controlled by the local needs of a tissue, whereas in the operant category, flow is controlled by needs of the organism and overall function of the tissue. In order to investigate the functional role of the repeating modular organization of cat mesenteric microcirculation, *in vivo* photomicrography and silicone injection methods were used to observe and analyze the microvasculature. The repeating module contains an area of membrane surrounded by a small artery and vein, an artery-to-artery and vein-to-vein continuity at the apices of the perimeter vessels, and subordinate order vessels represented by interior vessels of the unit [20]. Figure 3 shows the repeating module. From density measurements of all interior vessels of the injected preparations, it was found that density of vessels was in fact variable with respect to area, suggesting that distribution of the nutritional function is not directly related to the area of membrane. Since fat concentration is another important aspect of the mesentery, the same density measurements were performed in a cleared lean modular mesenteric unit to explain the density of internal vessels. The density of vessels was found to be less variable with respect to area in the lean unit, suggesting that the density of internal vessels is related to the quantity of fat in the membrane.

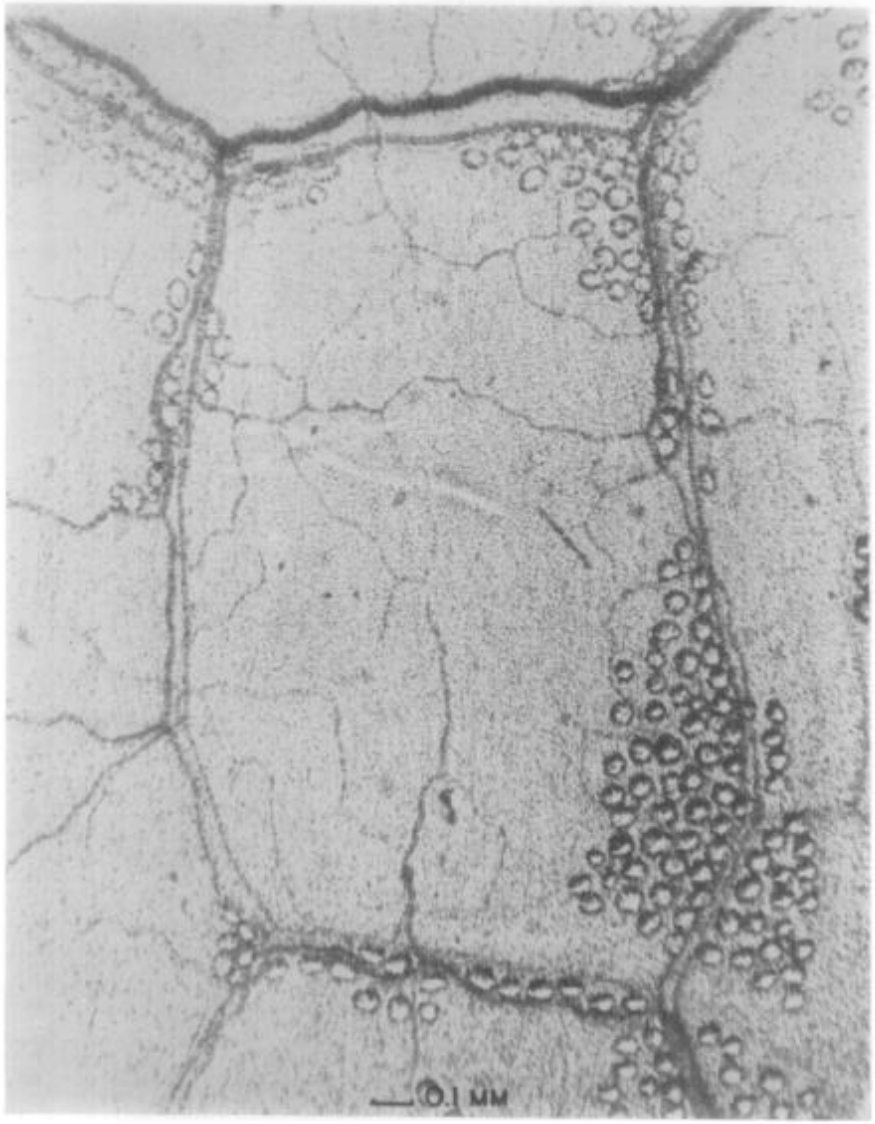

Figure 3: Single frame photograph of a module. [Reference 20: Frasher Jr. WG, and Wayland, H. A repeating modular organization of the microcirculation of the cat mesentery. *Microvascular Research* **4**: 62-76, 1972].

1.5 Skeletal Muscle: Rising Use as Microvascular Bed

For some time, the mesentery was often used in microvascular studies [56], [11], and [57], however, the use of skeletal muscle for microvascular observations began to make way. In 1964, R.T. Grant, who wished to explore the method of using skeletal muscle,

made direct observations of skeletal muscle blood vessels in the rat cremaster [23]. The skeletal muscle was suggested to be another ideal choice for microvascular studies, because the preparation allows for direct observations of vessels under different conditions. An example of this is presented in a comparison made by Bohlen et al. on microvascular pressures between normal and spontaneously hypertensive rats [9]. Observations and measurements were made on pressures, using a servo-null transducer, and diameters of both arteriolar and venular vessels at the same level of network in the cremaster muscle. Comparison of the microvascular pressures between normal and hypertensive rats is shown in Figure 4. Bohlen et al. showed that the increase in peripheral vascular resistance associated with hypertension is not influenced by vasoconstriction of microvessels in these cremaster preparations.

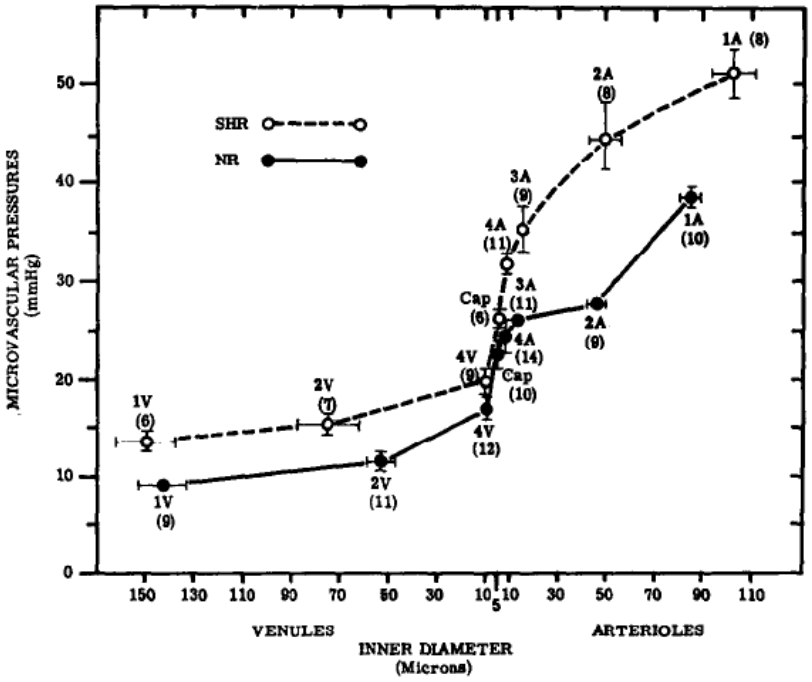

Figure 4: Microvascular pressures and diameters in the cremasteric muscle vasculature of normal (NR) and spontaneously hypertensive rats (SHR). The mean systemic arterial pressure in NR and SHR is 88.5 ± 2.1 and 115.6 ± 1.8 mmHg, respectively. The abbreviations above or below each data point refer to the branch order of the vessels; capillaries are designated by the abbreviation Cap. The numbers in parentheses refer to the number of observations on each branch order. Bars represent standard errors of the mean. [Reference 9: Bohlen HG, Gore, R.W., and Hutchins, P.M.

Comparison of microvascular pressures in normal and spontaneously hypertensive rats. *Microvascular Research* **13**: 125-130, 1977].

In building this support for skeletal muscles, Henriche and Hecke introduced detailed methods on their isolated rat gracilis muscle preparation and a discussion on its use in hemodynamic research and analysis [25]. Henriche and Hecke were able to demonstrate the advantage of gracilis muscle over other muscle preparations in terms of its ideal thinness and design for qualitative and direct quantitative analyses (blood flow and red cell velocity), as well as the surgical time required to prepare the tissue, which they found to be 20 – 30 minutes. The gracilis preparation is shown in Figure 5.

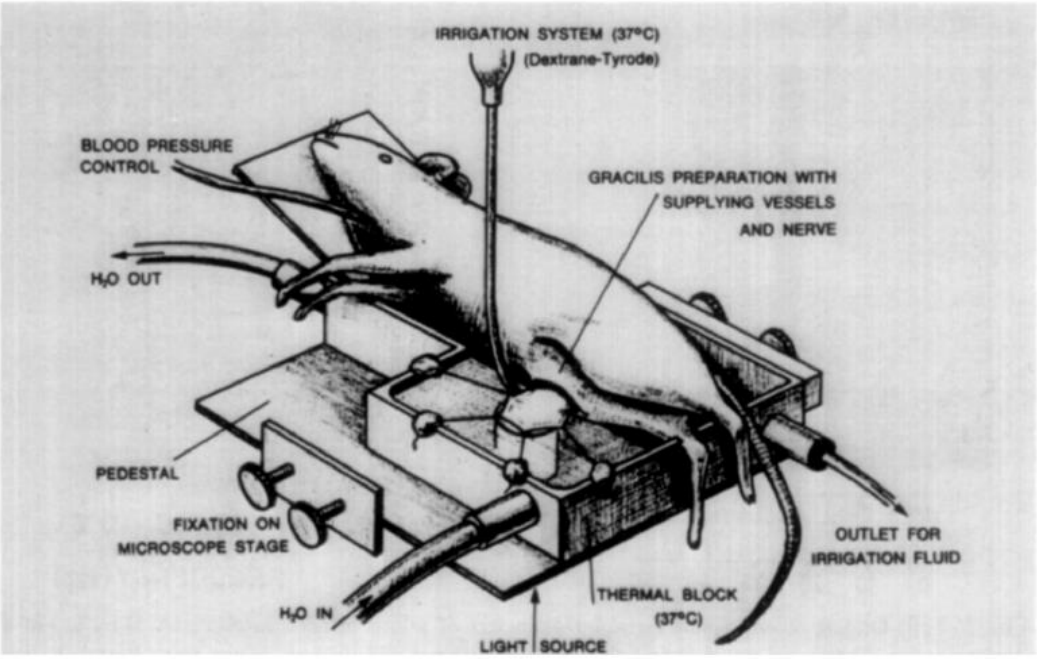

Figure 5: The gracilis muscle preparation mounted on a transparent tissue block and fastened by means of threads and Plasticine. During the experiments both the tissue block and the animal stage are temperature controlled (37º) by warm water. [Reference 25: Henriche HN, and Hecke, A. A gracilis muscle preparation for

quantitative microcirculatory studies in the rat. *Microvascular Research* **15**: 349-356, 1978].

1.6 Structural and Functional Quantification of Microvascular Networks

Thus far, the tools for studying structure and function of microvascular systems has allowed for both qualitative and quantitative descriptions and analysis. Zweifach and his colleagues made a big mark in network analysis at the time when they developed quantitative studies of microvascular structure and function. They quantified hemodynamic parameters such as pressures and velocities at various levels of networks in mesentery and omentum tissues [57]. In this study, Zweifach and Lipowsky aimed to compare micropressures and velocity at various vessels, and relate this to the topology of the network. Their experimental measurements were made using a Wiederhielm servo-null technique for micropressures and a two-slit photometric technique for intravascular pressures at both arteriolar and venular vessels ranging between 56 μm to 7 μm in size.

Shortly after, in 1980, Schmid-Schonbein et al. made another feat in microvascular research, where they described and used a method for measuring the cell distribution in capillary branches in the rabbit ear chamber [46]. Schmid-Schonbein et al. took measurements of flux and bulk flow for both red blood cells (RBCs) and white blood cells (WBCs) to obtain cell distribution functions for each. Figure 6 shows the distributions for one of the networks. They showed the nonlinearity of cell distribution and its dependence on the eccentric position of blood cells in capillary vessels. With their cell distribution function and a numerical simulation technique, Schmid-Schonbein et al. took a network-oriented approach and predicted path velocity, pressure drop, and concentrations of blood cells throughout a capillary network bed. It was shown that changes in velocity and pressure were due to the particle nature of blood rather than changes in resistance or diameter, as diameter remained constant.

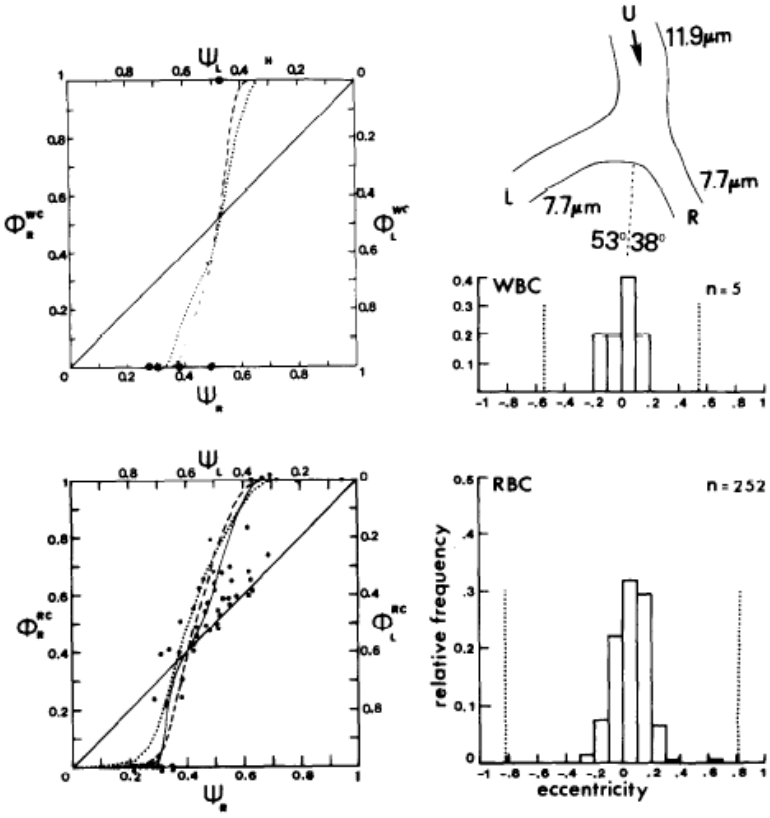

Figure 6: The cell distribution functions at a capillary bifurcation for WBCs (left top panel) and RBCs (left lower panel). The measurements are shown by the points and the solid line for Φ_R^{RC} represents a least-squares approximation. The dotted and dashed lines are theoretical predictions for a constant and parabolic velocity profile based on the eccentricity frequency distribution shown in the top right (white cells) and bottom right (red cells). The maximum possible eccentricity for a small WBC with diameter of 5 μm and a RBC with thickness 2.5 μm are indicated by the dotted vertical lines in the two distributions on the right-hand side. [Reference 46: Schmid-Schonbein GW, Skalak, R., Usami, S., and Chien, S. Cell distribution in capillary networks. *Microvascular Research* **19**: 18-44, 1980].

An essential aspect of understanding hemodynamics in a microvascular bed, and comparing such hemodynamics under different conditions, is the quantification of structural components. Engelson et al. supported this idea with their detailed analysis of the arteriolar network in the Wistar-Kyoto rat spinotrapezius muscle [15]. To observe the topological structure of the arteriolar microvasculature, the microvessels were perfused and filled with carbon to cause dilation, and therefore easy visualization. Figure 7 shows

the acquired montage and corresponding tracing for one spinotrapezius network. The spinotrapezius muscle was excised and observed under an intravital microscope, and the carbon-filled microvasculature was traced by hand on a transparent overlay [15]. The microvasculature begins with several feeding arterioles, which connect to form a meshwork of interconnecting or arcading arterioles. The arcading arterioles supply capillaries through transverse arterioles, which branch from arcade arterioles at regular intervals. In addition to qualitative descriptions, Engelson et al. also quantified the feeding and arcading arteriolar network with seven parameters, such as number of feeder arterioles, number of arcades in the meshwork, number of arterioles per arcade, number of bifurcations along the arcade perimeter, number of bifurcations inside the arcade meshwork. The branching topology and vessel geometry of the transverse arterioles were also quantified in their analyses.

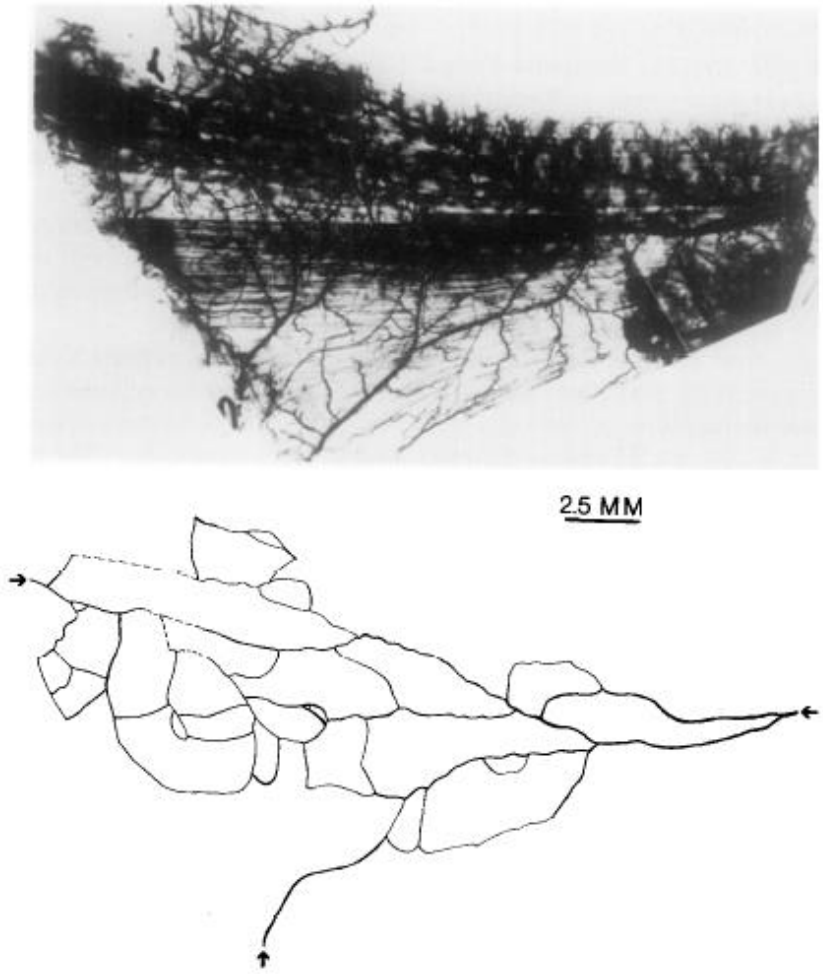

Figure 7: Microphotographic montage of a carbo-filled microvasculature in the spinotrapezius muscle of the rat. In the line drawing (bottom) the feeding and arcade arterioles are reproduced. The connections to the transverse arterioles as well as capillaries and venules are not shown for the sake of clarity. Diameters are not drawn to scale. The orientation of the muscle is as follows: right side, anterior end; left side, posterior end; top, lateral side; bottom, medial side along the spine. The three arrows indicate the feeding arterioles to the muscle. The feeder at the right is a branch from the brachiocephalic artery, the feeder at the top left connects to the 11^{th} intercostal artery, and the feeders at the bottom connects to an arcade artery in the underlying latissimus dorsi muscle and the 10^{th} intercostal artery. [Reference 15: Engelson ET, Skalak, T.C., Schmid-Schonbein, G.W. The microvasculature in skeletal muscle I Arteriolar network in rat spinotrapezius muscle. *Microvascular Research* **30**: 29-44, 1985].

Studies behind network-oriented analysis continued to develop throughout the 80s. A prominent group of researchers in Germany worked towards analyzing the topological structure of rat mesenteric microvascular networks [35]. Ley, Pries and Gaehtgens applied the Horton-Strahler scheme for ordering along with their own generation scheme to both arteriolar and venular networks in the rat mesentery. In order to gain a better understanding of the mesenteric microvascular growth pattern, Ley et al. used their topological analysis to assess the distribution of path lengths through vessel segments including arteriovenous vessels, which are vessels that directly connect an arteriole to venule.

In the same year, the same group of researchers continued their work in the rat mesentery, this time analyzing the hematocrit distribution across complete microvascular networks to observe and generalize the Fahraeus effect [41]. The Fahraeus effect explains the reduction of hematocrit in vessels that decrease in diameter [17], which is due to a velocity difference between red bloods cells and blood. In their analysis, Pries et al. presented the Fahraeus effect in the form of two different phenomena, vessel Fahraeus effect and network Fahraeus effect, which differ based on the RBCs and their velocities in question. Vessel Fahraeus effect explains the velocity profile and tube hematocrit reduction within a single vessel, whereas the network Fahraeus effect explains the difference in velocity and reduction in discharge hematocrit between two different vessels. To combine these two effects, Pries et al. developed and applied the concept of a total hematocrit reduction based on discharge hematocrit, tube hematocrit and diameters of vessel segments. The relative hematocrit for the vessel and network Fahraeus effect and total hematocrit reduction are given in Figure 8.

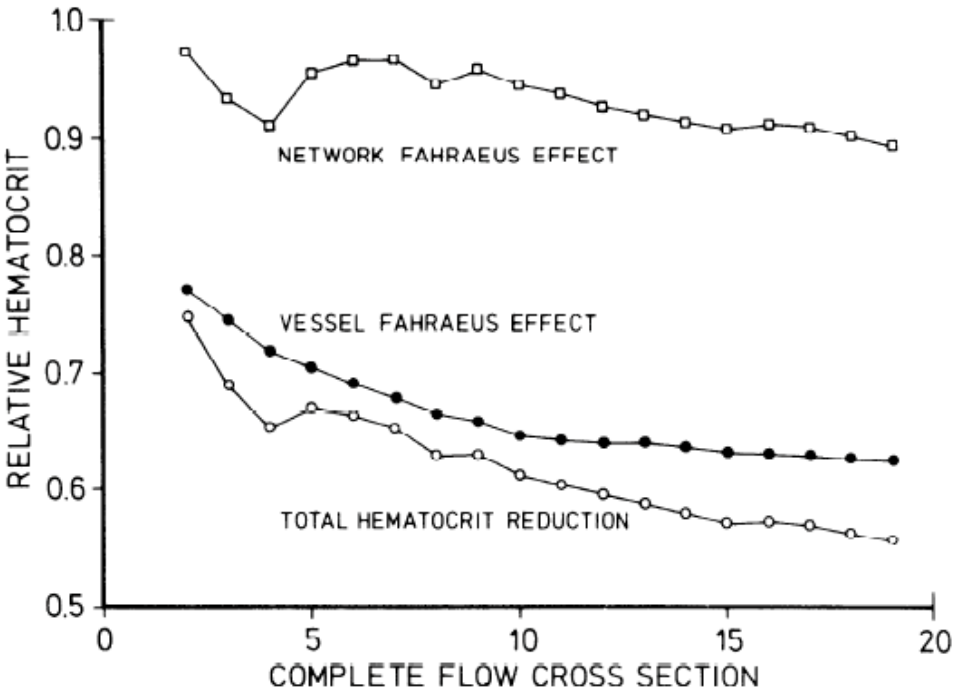

Figure 8: Contribution of vessel and network Fahraeus effects to total hematocrit reduction for consecutive-flow cross sections in 3 mesenteric microvessel networks. Hematocrit ratio given on *ordinate* is $\overline{H}_D^A \big/ H_D^*$ for network Fahraeus effect, $\overline{H}_T^A \big/ \overline{H}_D^A$ for the vessel Fahraeus effect, and $\overline{H}_T^A \big/ H_D^*$ for total hematocrit reduction, where $\overline{H}_D^A$ and $\overline{H}_T^A$ are the mean discharge and mean tube hematocrit of complete flow cross section weighted by individual cross-sectional areas, and H_D^* is the discharge hematocrit of arteriole feeding the network. [Reference 41: Pries AR, Ley, K., and Gaehtgens, P. Generalization of the Fahraeus principle for microvessel networks. *Am J Physiol Heart Circ Physiol* **251**: H1324-H1332, 1986].

1.7 Functional Dependence on Microvascular Structure

In all studies discussed so far on microvascular function, the structure of vessels and/or complete networks has played a necessary role in the quantification and comparison of hemodynamic parameters. This powerful concept of the influence of structure on function is the foundation for network analysis and was presented as such in a study by Ellsworth et al. in 1987. To facilitate accurate structural and functional analysis, Ellsworth et al. compared the two ordering schemes, centripetal and centrifugal, on

terminal arteriolar networks of the cheek pouch retractor muscle in young hamsters [14]. Their comparison was based on statistical analyses of the distribution of diameters and lengths with respect to vessel ordering, as well as the degree to which the ordering analyses obey Horton's laws. Between the two schemes, Ellsworth et al. found that centripetal ordering produced a significant difference between diameters and lengths in all adjacent orders, whereas the centrifugal ordering produced significant difference between only orders 3 and 4, and between orders 4 and 5. A depiction of the two ordering schemes applied to one network is shown in Figure 9. In terms of Horton's laws, which describe the relationship between order and mean diameter, mean length or number of vessels, Ellsworth et al. found that the associated diameter, length and bifurcation ratios were valid only for terminal vessels under centripetal ordering. In addition, Ellsworth et al. also analyzed the distribution of path lengths to assess the extent of network symmetry (or asymmetry), which can provide insight into the heterogeneity of microcirculatory flow patterns.

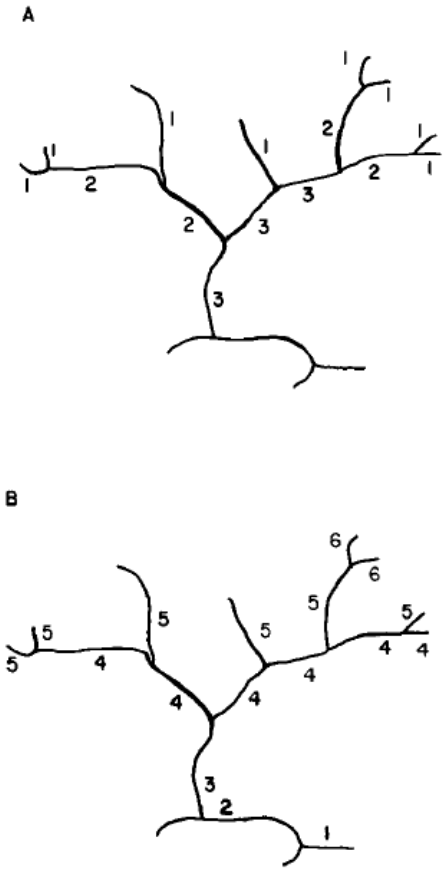

Figure 9: Diagrammatic representation of the two ordering schemes used in the present study applied to a terminal tree-like network. (A) Strahler ordering (note ordering was stopped at the third order in this network since further ordering required information on the vasculature downstream of the branch point along the main vessel. (B) Centrifugal ordering. [Reference 14: Ellsworth ML, Liu, A., Dawant, B., Popel, A.S., and Pittman, R.N. Analysis of vascular pattern and dimensions in arteriolar networks of the retractor muscle in young hamsters. *Microvascular Research* **34**: 168-183, 1987].

Network analysis continued to be an important aspect of microvascular research throughout the 80s and 90s. The desire to understand the essential relationship between microvascular structure and function was the driving force behind a network-oriented approach and was carried by the many prominent microvascular researchers already mentioned above. In 1996, Axel Pries, Timothy Secomb, and Peter Gaehtgens made a significant contribution to this understanding when they studied the effects of structural heterogeneity on network hemodynamics in the rat mesentery [42]. High variability and irregularity in geometrical parameters and topological structure of microvascular networks can be observed across different tissues. This high degree of structural heterogeneity can be influenced by the functional demands of a tissue, and therefore will determine how blood flows and RBCs are distributed through the network. In their study, Pries et al. measured geometry of rat mesenteric networks and applied this information to generate networks with varying levels of symmetry and regularity, based on the diameter, length and order of vessels. Schematics of the level of heterogeneity and irregularity in a given network are shown in Figure 10. Hemodynamic parameters were obtained through simulations of flow, and the effects of structural heterogeneity on these parameters were assessed. It was found that geometrical and topological heterogeneity does strongly influence hemodynamic parameters, such as pressure distribution, and mean and distribution of capillary hematocrit.

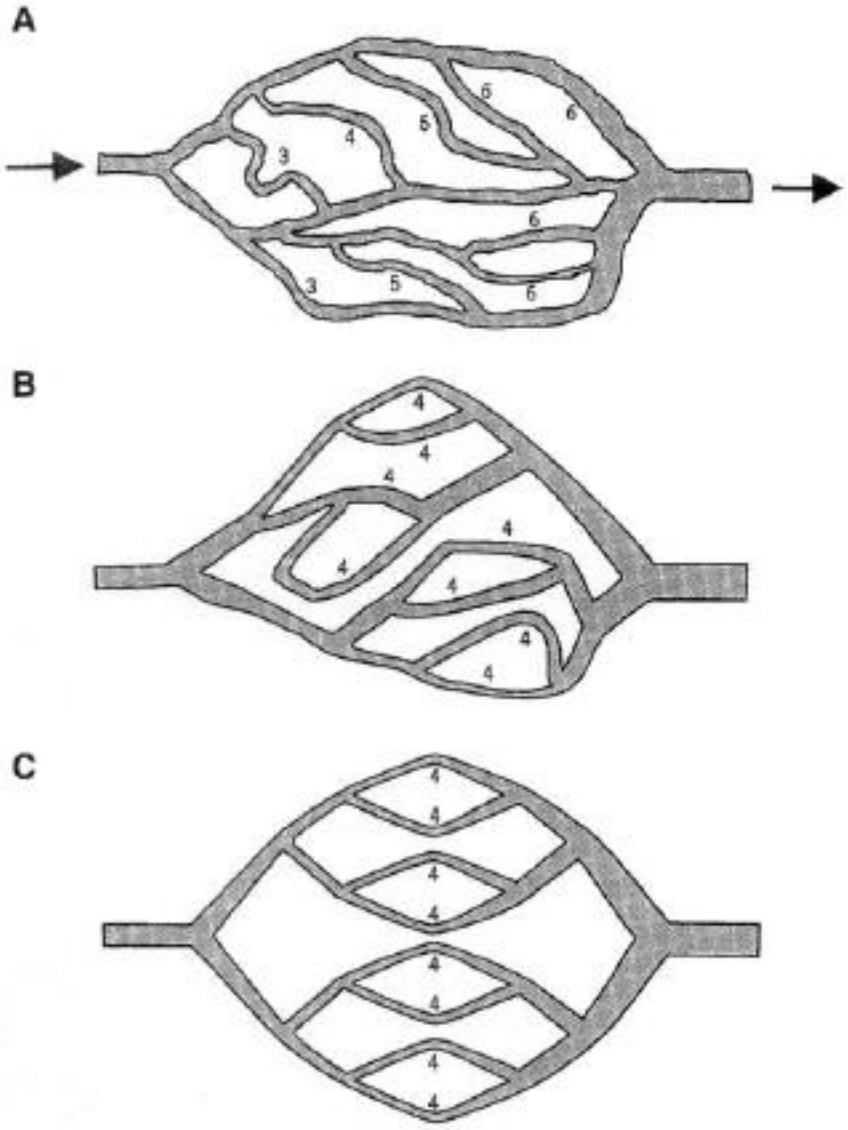

Figure 10: Schematic drawings corresponding to three network structures used in calculations. A: simplified schematic diagram illustrating an experimentally observed network with irregular morphology and irregular topology. As indicated, arterial generation no. of 9 capillary segments varies between 3 and 6. Vessel segments of any given generation no. exhibit different diameters and length. B: in symmetric irregular structure, topological structure is symmetric, and all 8 capillaries have same generation no. However, segment diameters and length are still variable. C: in symmetric regular structure, all segments of a given generation no. and type (arteriolar, capillary, venular) have same length and diameter. Because these values were obtained by averaging data from corresponding segments in observed structure, systematic diameter (and length)

differences between arteriolar and venular segments of same generation are maintained. [Reference 42: Pries AR, Secomb, T.W., and Gaehtgens, P. Relationship between structural and hemodynamic heterogeneity in microvascular networks. *Am J Physiol Heart Circ Physiol* **270**: H545-H553, 1996].

1.8 Theoretical Methods: Mathematical Modelling and Simulations

The development of network analysis and experimental techniques has necessitated the use and development of theoretical techniques, such as mathematical modeling. Obtaining physiological or hemodynamic parameters at every level or vessel in a single network is a very challenging and time-consuming feat, and therefore, has yet to be taken on. Fortunately, mathematical modeling solves this problem. A mathematical model is a set of mathematical equations, which describe the behaviour of a system. More specifically, the set of equations reflect the relationship between variables in the system and are used to predict the change in one variable given a change in another. In this way, hemodynamic parameters can be modeled by a set of equations, and therefore, be predicted at every level of a network with given conditions.

Some of the earliest models were developed in the early 1970s. In 1974, Gross et al. developed a network model for studying the pulsatile hemodynamics of the rabbit omentum microcirculation [24]. Their network model was based on pulsatile pressure and flow functions of geometrical and fluid mechanical properties of the microvessels. Pressure and red cell velocities were measured in select arterioles, capillaries, and venules using the servo-nulling system and dual-slit technique, respectively. In the network model, the microvasculature is simplified as levels of microvessel tubes of equal diameter connected in parallel. Numerical solutions for pulsatile pressure amplitude with changes in frequency (or heart rate) were obtained at each level of branching and compared to experimental results, which produced qualitative agreement. Pressure amplitude was also simulated for different physiological conditions, such as increase in length and compliance, and effects of vasodilator and vasoconstrictor. The intraluminal pressure and flow phase angle was also simulated across the microcirculatory bed at different frequencies. The results showed that there is a strong dependence on frequency

throughout the bed for pressure phase angle, and a dependence on frequency in the small artery and post-capillary sections of the bed for flow phase angle.

In the same year, Lee and Nellis presented a simple model for calculating the distribution of volume and flow in an idealized repeating modular system based on a cat mesenteric network. Lee and Nellis developed their flow and volume model with distributions of mean transit times (MTT), acquired using a microscopic dilution technique [34]. Measured dilutions produced computed MTT values, which describe the average time it takes a tagged indicator to travel from the mesenteric artery to the microvessel of interest. From the MTT and idealized repeating modular network, distributions of volume and flow through this network were computed. The distributions of MTT in a repeating module are shown in Figure 11.

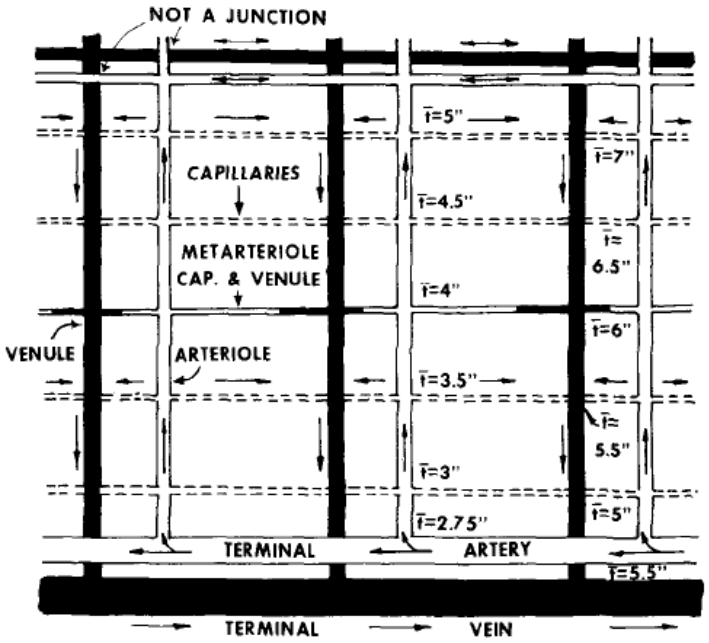

Figure 11: The vessel identification in a repeating module of the microcirculation of cat mesentery. The distribution of MTT, suggested from the microscopic indicator dilution experiment, is shown on the right hand side of the figure. The venous MTT is measured at a site just downstream of the junction. Note the adverse distribution of the MTT along the venule. [Reference 34: Lee JS, and Nellis, S. Modeling study on the distribution of flow and volume in the microcirculation of cat mesentery. *Annals of Biomedical Engineering* **2**: 206-216, 1974].

A few years later in 1978, Lipowsky et al. aimed to acquire the distribution of blood rheological parameters in the microvasculature of the cat mesentery [37]. Using measured diameters as the index of position, distributions of intravascular pressure gradients were measured with a dual micropressure system in arteriolar, capillary and venular vessels ranging from 7 to 58 μm. Simultaneous measurements of red cell velocity were made with two-slit photometric technique. Intravascular hematocrit was also measured for vessels with diameters less than 15 μm. Mathematical relations were used to compute intravascular wall shear stress and apparent viscosity, given pressure and bulk velocity. From their *in situ* measurements and computations, Lipowsky et al. found that pressure gradients, wall shear stress and velocity were lower in venules compared to arterioles at the same level of network, whereas apparent viscosity was higher in venules than arterioles. Furthermore, Lipowsky et al. used their measured data to compute resistance across the cat mesenteric network and showed an increase in resistance across arterioles and a mirrored decrease in resistance across venules.

Pries et al. demonstrated the power of mathematical models in 1990, when they developed and described a theoretical model for simulating blood flow in microvascular networks [43]. Their model is based on measured structural parameters and relations describing rheological behaviour in microvascular networks, such as the Fahraeus effect, Fahraeus-Lindqvist effect, and the phase separation phenomenon. The structure of the microvascular network is divided into nodes and connecting segments, which represent sections of vessels through which hemodynamic and rheological parameters are computed. Given apparent viscosity in each vessel segment, as well as inflow and outflow boundary conditions in the form of flow or pressure, the flow in each internal segment and pressure at each node is computed in the first procedure of the numerical computation technique. Next, in the second procedure, pressure and flow at every segment become the inputs for computing discharge hematocrit. To assign the distribution of hematocrit across these vessels, the phase separation relation describing the distribution of red blood cells and plasma at bifurcations is employed. With discharge hematocrit, apparent viscosity and tube hematocrit can be computed using the Fahraeus-Lindqvist effect and Fahraeus effect, respectively. The apparent viscosity is then fed back into the first procedure to obtain a second iteration of flow and pressure,

which is used to obtain viscosity and hematocrit, and so on. The procedures are alternately repeated in iterations until the numerical values converge. To validate their mathematical model, Pries et al. measured hematocrit at all vessel segments in two different sized networks (large and small) and compared them to model predicted values. Their results for hematocrit distributions showed close agreement between predicted and measured values.

1.9 Network Analysis: A Powerful Microvascular Tool

The aim of our historical review is to reemphasize the importance of the network-oriented approach in microvascular research. Our argument is supported by influential studies described thus far and echoes the strong argument made by Peter Gaehtgens in favour of network-analysis in 1992. In his paper titled 'Why Networks', Gaehtgens discusses the challenges associated with studying the behaviour of a microvascular system, and why a network or integration-approach is a step towards an accurate understanding of this behaviour [21]. To start, Gaehtgens highlights the most significant feature of the microcirculation, which is that its hemodynamic behaviour is different from that of the macrocirculation. The combination of a complex, asymmetric microvascular structure and the particulate nature of flowing blood make it difficult to estimate the behaviour of blood flow in the microcirculation with measurements at the macrocirculation. A consequence of this observed discrepancy between micro- and macro-circulatory behaviour is the discovery of microcirculatory flow heterogeneity, shown in the wide dispersion of intravascular pressures and volume flows, which has been before explained by the architectural complexity of microvascular structure and the particulate behaviour of blood flow. It is, therefore, not accurate to assume that changes in total blood flow at the tissue level will agree with changes at single vessels.

The aim to quantify functional parameters at a given level requires a proper classification of vessels, which, Gaehtgens explains, cannot rely purely on architectural or topological classification of vessels or on an exclusive functional definition. The reason for this is that there is considerable overlap in function between vessels at different levels of the network. For example, it has been shown that post-capillary venules are also involved in exchange of substances between blood and tissue, which is known to be the main

function of capillary vessels. In addition to the overlap in function, it has been shown that vessel segments communicate by a variety of mechanisms, such as chemical and/or electrical signals and transmission of substances, which makes it difficult to associate a response or function with a single vessel segment. As a result of vessel communication, there exists a close coupling of vessels in a network and a strong interdependence of control mechanisms, such as myogenic and metabolic. Microcirculatory responses to changes in physiological environment would, therefore, be integrated rather than isolated or localized, and thus the study of microcirculation would require a network approach that describes the microcirculation as an integrated system rather than a collection of interrelated segments. Most studies currently applying the network approach aim to understand and describe the distribution of hemodynamic parameters such as intravascular pressures, flow velocities or hematocrit, and include quantitative analysis of network structure and function using mathematical network modeling techniques. Mathematical modeling based on known geometry and blood rheology has shown to be a reliable method for closely predicting distributions of hemodynamic parameters.

As a further expansion of network analysis, the effects of changes in overall blood flow on tissue perfusion in conditions such as hyperemia or hypoxia should be considered. It is shown that heterogeneity of microvascular networks gives rise to non-uniform distribution of cells and plasma, which leads to a variability at the capillary level in red cell concentration, and therefore exchange. Since flow heterogeneity is known to effect exchange efficiency, the relationship between network heterogeneity and total flow regulation is of great interest [21].

1.10 With all These Great Developments, What's left to do?

Due to the inverse power law, describing the relationship between arteriolar diameter and resistance, studies measuring only arteriolar radius at bifurcations have dominated skeletal muscle blood flow research. Microvascular studies using IVVM (*in vivo*) or isolated vessels (*in vitro*) commonly investigate local arteriolar regulation/dysregulation in isolated arterioles or at one or more arteriolar bifurcations. Although data from such

studies have shaped our understanding of microvascular control, the contribution of local arteriolar responses to overall changes in network resistance, blood flow, and RBC distribution is commonly left to speculation or inference. For decades, theoretical modeler's have stressed that quantitative analysis of the distribution of microvascular blood flow and hematocrit requires a detailed description of the vascular network geometry [14]. In fact, hemodynamic characteristics of heterogeneous microvascular networks can only be adequately described if both topological and geometric variability in network structure are considered [42].

Building on the "network concept", we have shown that the degree to which each sympathetic ligand modulates arteriolar segmental resistance is dependent on arteriolar order (i.e., topology) in complete branching networks [4]. Like others, we have shown that α_1- and α_{2-} adrenergic receptor control is greatest at large (1^{st} and 2^{nd} order) arterioles, with declining sensitivity in subsequent branch orders approaching capillary beds [16,27]. Beyond this, we have observed that NPY and ATP elicit the greatest constrictor effects in arterioles closest to capillaries, with declining effects in ascending branch orders approaching feed arterioles. Based on these findings, we are the first to illustrate that spatial differences in ligand sensitivity enable the SNS to modify bulk tissue blood flow and RBC distribution differentially in branching networks [4].

Since arteriolar network geometry and topology play a considerable role in setting network resistance and distributing hematocrit, it then follows that acute control of vasodilation and vasoconstriction would coordinate with network geometry and topology to efficiently regulate blood flow and RBC distribution in heterogeneous microvascular networks. However, up until recently the limitations offered by IVVM models of skeletal muscle blood flow have not been ideal for this initiative. Since 2012, our group has been revolutionizing the way we study and understand microcirculatory function and control. The remainder of this review highlights, what we feel, are the current technical challenges that limit a detailed and comprehensive understanding of microvascular rheology from a network perspective. As challenges are presented, we have provided solutions based on our validated approaches.

1.10.1 Development of an Ideal Experimental Model to Comprehensively Describe Blood Flow Rheology in Skeletal Muscle Microcirculatory Networks

Blood flow throughout microvascular networks involves complex alterations in fluid dynamics and depends on the topology of the network you are interrogating. Although commonly overlooked, this complexity is due to well-understood physical principles that must be considered when describing the divergent nature of flow of viscous multiphase fluids, through bifurcating networks of microvessels, with progressively decreasing tube diameters. Compound this with the fact that microvascular sensitivity to vasoactive pharmacological agents displays robust topological dependency and it becomes apparent that the development of new experimental models and tools is needed to accurately measure microvascular network rheology.

One of the greatest limitations to understanding microvascular rheology from a network perspective is the lack of an ideal experimental model. The first requirement for an ideal experimental model for a network approach using the conventional IVVM would be planar geometry, to enable rapid acquisition of microvascular data in a single focal plane. The second requirement is that the skeletal muscle of interrogation must be physiologically, functionally, biomechanically, and metabolically relevant to locomotive skeletal muscle. Third, the experimental preparation must include access to the muscle, for field stimulation, and the entire microvascular network for drug delivery via superfusion and/or micropipettes (for microiontophoresis or "picospritz" pharmacology). Fourth, the experimental model must be compatible among males and females, to enable studies involving understanding sexual dimorphism.

Up to the gluteus maximus muscle (GM), there was not a model we deemed ideal for our studies. Other models have limitations, for example, the cremaster, which is sex dependent, and the cheek pouch, which is not locomotive. Currently, the only model that satisfies all of the aforementioned criteria is the gluteus maximus muscle (GM) preparation for IVVM. First developed in C57BL/6 mice in Steven Segal's lab in 2004

[6], we have significantly refined this model and currently use it to study many different strains of mice and rats.

1.10.2 Overcoming Challenge 1

Challenge 1: How to measure blood flow in fast flowing arteriolar networks.

Solution: A simple "streak length method" for quantifying and characterizing red blood cell velocity profiles and blood flow in rat skeletal muscle arterioles [3].

Most studies (current and past) use the product of mean RBC flow velocity (V_{Mean}) and vessel cross-sectional area (A_{Vessel}), which is derived from centerline V_{RBC} (V_{Center}). For decades, direct optical measures of centerline velocity in microvessels have been accomplished using Doppler velocimetry [28,52] or the dual-slit/sensor technique [33,44]. In an effort to calculate blood flow from such techniques, V_{Center} is converted to V_{Mean} through the use of the Baker and Wayland velocity ratio conversion factor 1.6 ($V_{ratio} = V_{centre} / V_{mean}$) ; which serves as an estimate of V_{RBC} profile bluntness and transition layer. However, the use of 1.6 as a constant in blood flow calculations disregards notable diameter- and Hct-dependent changes in luminal V_{RBC} profiles that occur across a range of microvascular diameters. The erroneous use of a constant introduces significant systematic errors that over- or under-estimate blood flow. Prior to the innovation and validation of the *Streak-Length Method,* our understanding of arteriolar V_{RBC} profiles in skeletal muscle were limited to data collected from arterioles and venules in the mesentery [38,49-51] and omentum, [45], or skeletal muscle venules [7,12].

At present, the evaluation of microvascular V_{RBC} profiles is limited to experiments investigating arterioles and/or venules in the mesentery [38,49-51] and omentum [45], or skeletal muscle venules [7,12]. However, due to experimental and technical limitations, these past studies have been constrained to a small range of arteriolar diameters (approximately 17–40 μm), limiting current knowledge of V_{RBC} profiles to this range.

Arteriolar networks in many tissues have a broad range of diameters; for example, skeletal muscle arterioles range from ~15 to ~100 μm. Thus, there remains a need for a feasible *in vivo* experimental model enabling concurrent measurement of V_{RBC} profiles at multiple levels within microvascular networks. Having a means to acquire V_{RBC} profiles for a broad range of arteriolar diameters would provide accurate and detailed data necessary to derive V_{Ratio}. Such data would facilitate accurate blood flow calculations for a broad range of arteriolar diameters in studies limited to centerline V_{RBC} measurements that require V_{Ratio} to calculate V_{Mean}.

In this study, we developed and validated a novel *in vivo* method for characterizing V_{RBC} profiles, V_{Ratio}, and blood flow in arterioles with a broad range of diameters from microvascular networks in rat skeletal muscle (Figure 12). Furthermore, we derived a linear relationship between V_{Ratio} and arteriolar diameters (from 21 to 115 μm) (Figure 13). From this relationship, we have derived an equation that may be used in other studies to calculate blood flow based on the arteriolar diameter of interest. This work provides significant insight to the field of blood flow and single RBC dynamics in complete microvascular networks.

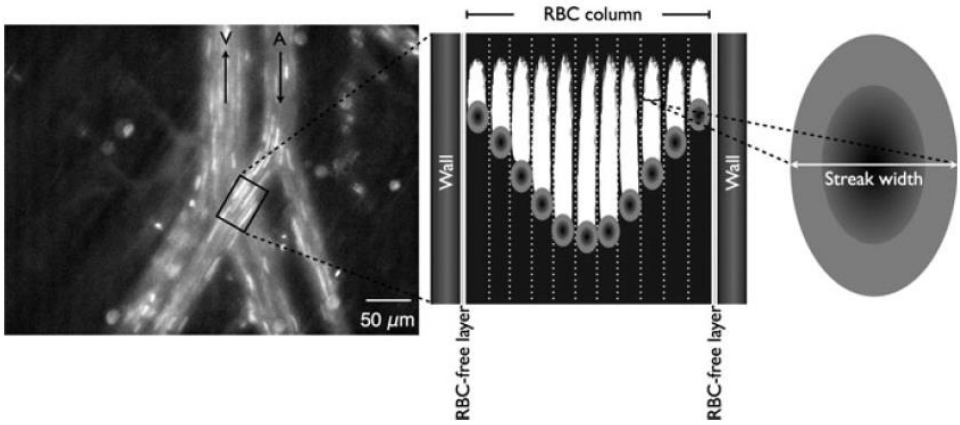

Figure 12: Schematic of streak length method technique. Epi-fluorescent image of an arteriolar (A) and venular (V) bifurcation in the rat gluteus maximus muscle (🡻: direction of flow); exposure time: 10 milliseconds; 15 fps at 10x. Arteriolar lumen was divided into "lanes" based on the number of RBCs spanning the RBC column, with RBC width represented by streak width. [Reference 3: Al-Khazraji BK, Novielli NM, Goldman

D, Medeiros PJ, Jackson DN. A simple "streak length method" for quantifying and characterizing red blood cell velocity profiles and blood flow in rat skeletal muscle arterioles. *Microcirculation* **19**: 327-335, 2012].

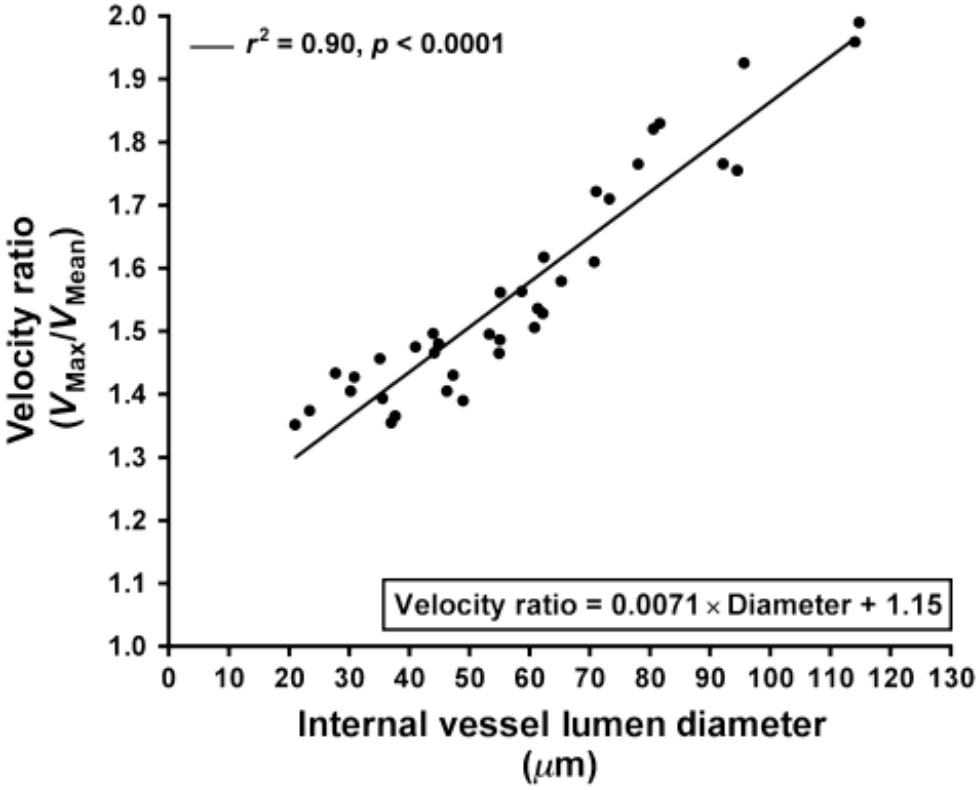

Figure 13: Relationship between velocity ratio and arteriolar diameter. Velocity ratios for arterioles with diameters ranging from 21 to 115 µm (5-10 arterioles per animal; n=6 animals). Within all animals, there was a positive correlation between diameter and V_{ratio} (mean r^2 = 0.90; $p < 0.0001$). For all data, the velocity ratio, as a function of arteriolar diameter (in µm), is described by the experimentally derived equation shown below the graph. [Reference 3: Al-Khazraji BK, Novielli NM, Goldman D, Medeiros PJ, Jackson DN. A simple "streak length method" for quantifying and characterizing red blood cell velocity profiles and blood flow in rat skeletal muscle arterioles. *Microcirculation* **19**: 327-335, 2012].

1.10.3 Overcoming Challenge 2

Challenge 2: How to measure WSR in microcirculatory networks.

Solution: A Microvascular Wall Shear Rate Function Derived From *In Vivo* Hemodynamic and Geometric Parameters in Continuously Branching Arterioles [2].

Transmural pressure gives rise to forces exerted on the vessel wall, such as circumferential and longitudinal stress. Shear stress, a tangential force under laminar flow conditions, occurs due to the viscous interaction of cellular laminae flowing past one another at different velocities, and when blood flows along the vessel wall, the friction results in wall shear stress. Wall shear stress elicits mechanotransduction along the endothelium resulting in flow-mediated vasodilation, an integrated response which is important for healthy vasoregulation [32]. Endothelium-dependent flow mediated dilation has been shown to be integral to adequate blood perfusion in the microcirculation of skeletal muscle [8], [13], [30].

Wall shear stress is the product of blood viscosity and WSR, where WSR is defined as the radial velocity gradient in the cell free plasma layer (i.e., CFL), which is encompassed by the velocity profile. In the experimental setting and under the assumption of steady plasma flow and a linear slope in the velocity profile through the CFL, the WSR equation is defined as the difference between the edge velocity of the red blood cell column (V_{EDGE}) and velocity at the wall (V_{Wall}) over the CFL width: $\gamma_E = \frac{V_{\mathrm{EDGE}} - V_{\mathrm{Wall}}}{Width_{\mathrm{CFL}}}$. Satisfying the no-slip condition, where V_{Wall} is zero, this equation becomes $\gamma_E = \frac{V_{\mathrm{EDGE}}}{Width_{\mathrm{CFL}}}$.

Experimentally obtaining the edge and CFL velocities necessary to accurately compute WSR is difficult and time consuming. Thus, many groups have commonly quantified shear rate from experimentally derived mean blood velocity (V_{Mean}) and arteriolar diameter (D), using the equation: $\gamma_{\mathrm{Wall}} = \frac{8\, V_{\mathrm{Mean}}}{D}$. V_{Mean} is routinely calculated by dividing maximum velocities V_{Max} by a velocity ratio (V_{Ratio}) constant that assumes velocity profile shape: $V_{\mathrm{Mean}} = \frac{V_{\mathrm{Max}}}{V_{\mathrm{Ratio}}}$. The commonly used velocity ratio of 1.6 was first implemented by

Baker and Wayland [5] to account for spatial averaging artifacts associated with using the dual sensor velocimeter instrument for acquiring centerline red blood cell velocities.

However, the use of a velocity ratio of 1.6 is only acceptable where lateral averaging of velocities is absent, the relative size of the sensor to the vessel diameter is known, and the velocity profile is purely parabolic in nature [40]. As such, we previously investigated the validity of maintaining a constant velocity ratio across all arteriolar diameters in microvascular networks [3]. In this past study, we acquired *in vivo* RBC velocity profiles from continuously branching arteriolar trees arteriolar spanning the *in situ* gluteus maximus skeletal muscle preparation and reported that RBC velocity ratios were dependent on arteriolar diameters, (for details see *Challenge 1* above [3]).

As WSR is the slope of the velocity profile evaluated at the wall, the velocity profile data from our previous study [3] can be used to calculate WSR. Although a limited number of studies report calculating shear rate values from velocity profiles, these past data are limited to narrow ranges of diameters as shown in exemplary studies where data were obtained from the mesenteric microcirculation (17–32 μm) [49] or from random sites of observation in the rat cremaster muscle [39], or estimated from computational simulations [47]. To date, γ_E values from experimentally derived velocity profiles in complete, continuously branching, skeletal muscle arteriolar trees have not been calculated.

Thus, using the rat GM, adapted from the mouse [6] and our "streak length" method for measuring luminal RBC velocity profiles in continuously branching arteriolar trees [3] , we concluded [2]:

(i) Estimated WSR calculated from experimentally acquired velocity profiles are independent of arteriolar diameter; (ii) a straightforward WSR equation has been derived from the relationship of experimental hemodynamic parameters with arteriolar diameter, and this equation yields WSR calculations that are similar to our experimental values (Figure 14), (iii) our estimated WSR (Figure 15), γ_E, was significantly greater than WSR values evaluated under Poiseuille parabolic flow assumption, regardless of the velocity ratio value (Figure 16).

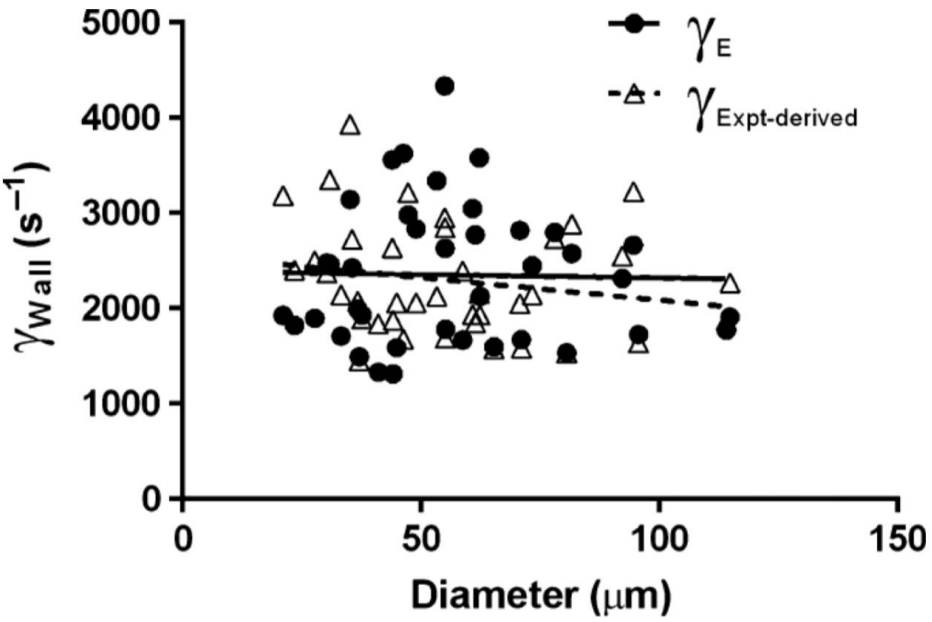

Figure 14: Comparison of experimental and calculated WSR. Comparison of estimated WSR from experimentally derived velocity profiles γ_E, 2350 ± 117.3/sec (mean ± SEM across all diameters), versus calculated WSR from the experimentally derived equation, $\gamma_{Expt-derived}$, 2291 ± 93.6/sec (mean ± SEM across all diameters). Calculated $\gamma_E$were similar between the two methods (comparison of means using paired *t*-test), and each set of $\gamma_E$values had no relationship with diameter. r^2 for γ_E is 0.0005; r^2 for $\gamma_{Expt-derived}$ is 0.04. [Reference 2: Al-Khazraji BK, Jackson DN, Goldman D. A Microvascular Wall Shear Rate Function Derived From In Vivo Hemodynamic and Geometric Parameters in Continuously Branching Arterioles. *Microcirculation* **23**: 311-319, 2016].

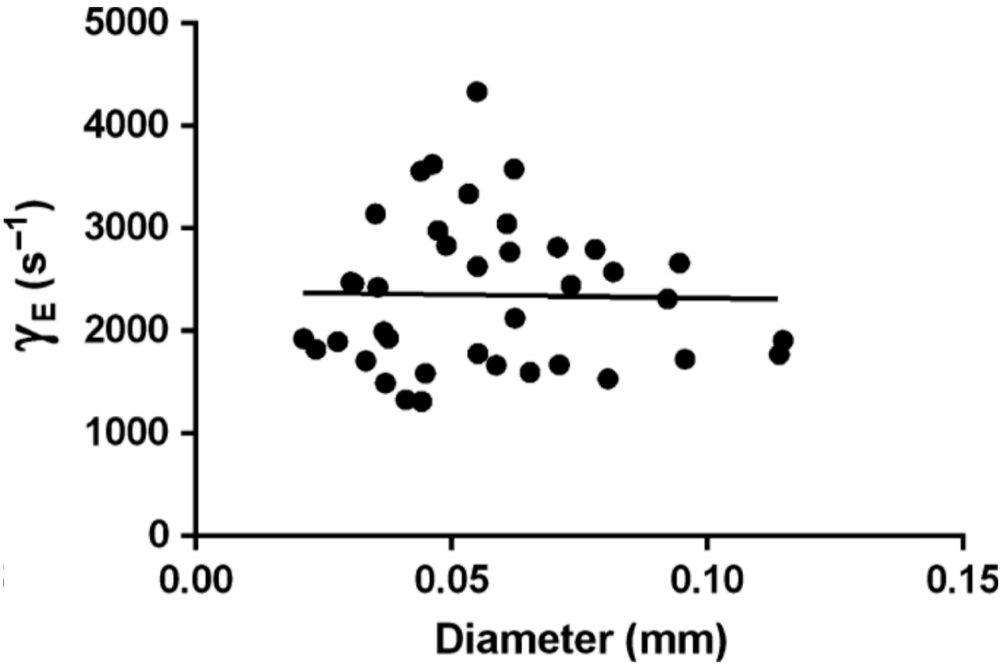

Figure 15: Relationship between experimentally acquired γ_E and arteriolar diameter. Calculated γ_E values (using edge velocities) as a function of arteriolar diameter. Calculated experimental γ_E were independent of arteriolar diameter γ_E values, ranging from 1317 to 4334/sec, for arteriolar diameter ranging from 0.021 to 0.115 mm. [Reference 2: Al-Khazraji BK, Jackson DN, Goldman D. A Microvascular Wall Shear Rate Function Derived From In Vivo Hemodynamic and Geometric Parameters in Continuously Branching Arterioles. *Microcirculation* **23**: 311-319, 2016].

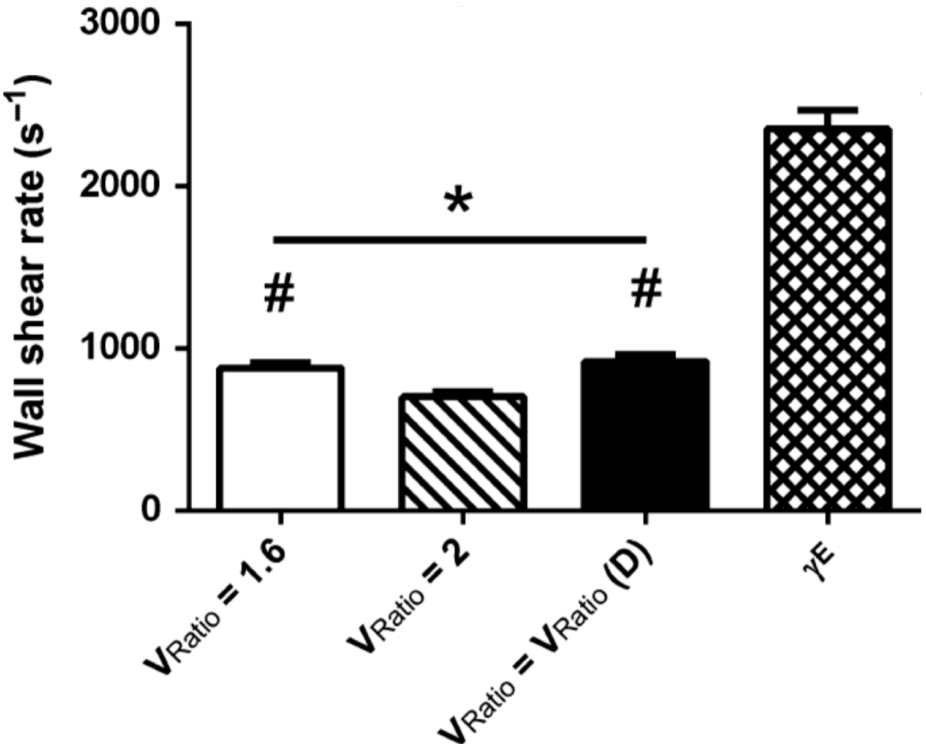

Figure 16: Comparison of WSR using different velocity ratios. WSR results for (i) experimental WSR, 2350 ± 117.3/sec, (ii) $V_{\mathrm{Ratio}} = 1.6$, 877.6 ± 35.6/sec, (iii) $V_{\mathrm{Ratio}} = 2$, 702.1 ± 28.48/sec, and (iv) $V_{\mathrm{Ratio}}(D) = 0.0071 \times (D) + 1.15$, 917.6 ± 43.5/sec (mean ± SEM across all diameters). *indicates different from γ_{E}, and #indicates different from $V_{\mathrm{Ratio}} = 2$, ($p < 0.05$). Data presented as mean ± SEM across all diameters. [Reference 2: Al-Khazraji BK, Jackson DN, Goldman D. A Microvascular Wall Shear Rate Function Derived From In Vivo Hemodynamic and Geometric Parameters in Continuously Branching Arterioles. *Microcirculation* **23**: 311-319, 2016].

1.10.4 Overcoming Challenge 3

Challenge 3: Develop IVVM procedures and tools for *in vivo* collection and analysis of complex microvascular networks.

Solution: Comprehensive In Situ Analysis of Arteriolar Network Geometry and Topology in Rat Gluteus Maximus Muscle [1].

Our methods to quantitatively analyze the distribution of arteriolar blood flow and hematocrit in the rat gluteus maximus (GM) muscle has continued to develop over the past few years. Our technique begins with a comprehensive geometric analysis of complete arteriolar networks, which was conducted by Mohammed Al Tarhuni [1]. In his study, Tarhuni analyzed geometrical and topological parameters in 8 different rat GM muscle networks *in situ* under baseline conditions and compared them to assess heterogeneity across. The experiments involved a GM preparation observed under an intravital video microscope (IVVM). The rat GM preparation was developed in our lab and is the model choice for skeletal muscle hemodynamic studies due to its planar geometry and uniform thinness, which allow imaging access to the entire microcirculation within a single focal plane. The IVVM images were registered in Matlab to create a complete photomontage of the arteriolar network. Topological reconstruction of the microvascular network involved registering nodes approximately 150 μm apart along unbranched arteriolar segments. The diameter and lengths of segments were measured using ImageJ and input into a centrifugal ordering algorithm in Matlab to generate arterioles with orders ranging from 1^{st} to 9^{th} order. The centrifugal algorithm assigns the main feed arteriolar an order of 1 and assigns higher order to daughter vessels that have diameters less than 80% of the parent and/or bifurcation angles greater than 15%. Mean diameter and lengths were calculated for arteriolar elements, which are defined as a group of segments connected serially of the same order [1]. The level of symmetry of a given topological order can be calculated from an average segment-to-element ratio (S/E). In addition, fractal dimensions were calculated using the box-counting method in *FracLac*.

The relationship between the geometry and order, given our ordering scheme, was analyzed. The mean internal vessel lumen diameters and mean vessel element lengths were plotted and showed to decrease with increasing topological order, while the number of elements increased with increasing topological order (Figure 17). This data was further analyzed to calculate diameter, length, and bifurcation ratios to test the validity of

Horton's laws in the arteriolar network. The bifurcation ratios are obtained from the slope of the regression line between the logarithm of each diameter, length or number of vessels and topological order. Three different methods for calculating the geometric ratios of each network were also compared. The strong linear fits ($R^2 \geq 0.9$) indicate that the Horton's laws are obeyed within the arteriolar networks of the rat GM. The geometric ratios were also used to predict mean values of the diameter, length, and number of elements from measured 1^{st} order values. The comparison between predicted and observed values showed that the bifurcation ratios can closely predict these geometric parameters at every order.

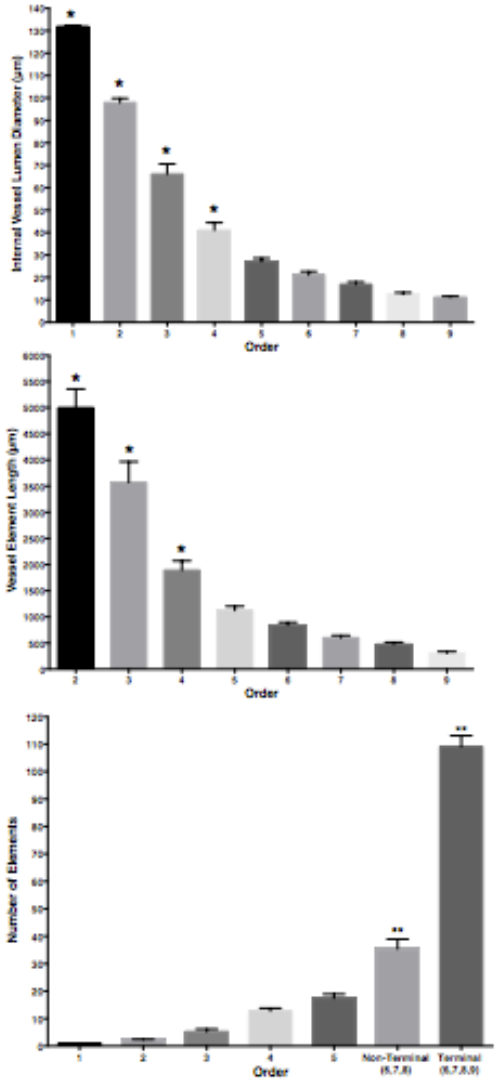

Figure 17: Relationships between mean internal luminal diameter (top), vessel element length (middle), and number of elements (bottom) and order. Mean diameter and length decreased with increasing topological order, while number of elements increased with increasing topological order. Data presented as mean ± SEM (n=8 animals). (* significantly different from subsequent order at $p < 0.05$, ** significantly different from previous order at $p < 0.05$). [Reference 1: Al Tarhuni M, Goldman D, Jackson DN. Comprehensive In Situ Analysis of Arteriolar Network Geometry and Topology in Rat Gluteus Maximus Muscle. *Microcirculation* **23**: 456-467, 2016].

Geometry of arteriolar networks was further analyzed for variability within a single network (intra-network) and between different networks (inter-network). We found

lower levels of heterogeneity in terms of mean diameter and length between networks than within networks, implying a relatively high geometrical and topological similarity between networks. The maximum level for both intra- and inter-network heterogeneity was typically found to be at orders 5 and 6. Furthermore, the symmetry analysis showed that the S/E ratio was highest, most asymmetric, at orders 3 and 4. The final analysis was that of fractal dimensions, which were obtained to compare the overall structure of the 8 different arteriolar networks. Fractal dimensions provide a measure for network structural complexity, and were found to range between 1.3315 and 1.4202, with a coefficient of variation (CV) of 1.86%, which implies little structural variability between the networks.

1.10.5 Onto Challenge 4

Challenge 4: Integration of experimental data from arterioles and venules to predict hemodynamic outcomes.

Solution: *Chapter 2* - Optimizing arteriolar network hemodynamic analysis using an integrated model derived from experimental data.

Since a detailed description of microvascular network geometry is critical to make accurate and meaningful predictions of rheological outcomes, we have spent over 8 years developing and validating the experimental tools described above. By using an iterative approach, whereby our experiments drive the evolution of our theoretical model, several interesting and novel rheological phenomena have "organically" emerged. In order to utilize complex and heterogeneous experimentally derived microvascular network data for accurate theoretical modeling, one must seriously consider (at least) two fundamental principles: 1) the overall pressure drop across the network (which informs us that network resistance is accurate), and 2) the Murray's Law exponent (which informs us that network structure is accurate). Fundamentally, Murray's Law is a calculation of "network efficiency" and describes the power relationship between the flow of a fluid (e.g., the blood) and diameter of conduits within which the fluid is flowing (e.g., the arteriolar

network of interest). Essentially, Murray's law is key to this relationship, where an exponent of 3 is considered "ideal" in terms of efficiency. If our arteriolar networks obey Murray's law, then the assumption is that the network is optimized for efficiency.

As such, in the following study we address the impact of including variable capillary resistance and measured venular network geometry, on the integrated accuracy of: 1) Murray's law, and 2) well-established values for pressure drops across microvascular networks. We begin by reconstructing several experimental arteriolar networks and the corresponding venular networks. Next, we develop tools for connecting the arteriolar and venular networks, for adding the resistance of capillaries and smaller arterioles and venules, and for computing hemodynamic properties of the combined arteriolar-venular networks. We then validate these methods by applying them to a reconstructed network for which blood flow data was obtained using the streak length method. Finally, we demonstrate the utility of these methods by applying them to a set of reconstructed networks to determine their hemodynamic properties.

1.11 References

1. Al Tarhuni M, Goldman D, Jackson DN. Comprehensive In Situ Analysis of Arteriolar Network Geometry and Topology in Rat Gluteus Maximus Muscle. *Microcirculation* **23**: 456-467, 2016.

2. Al-Khazraji BK, Jackson DN, Goldman D. A Microvascular Wall Shear Rate Function Derived From In Vivo Hemodynamic and Geometric Parameters in Continuously Branching Arterioles. *Microcirculation* **23**: 311-319, 2016.

3. Al-Khazraji BK, Novielli NM, Goldman D, Medeiros PJ, Jackson DN. A simple "streak length method" for quantifying and characterizing red blood cell velocity profiles and blood flow in rat skeletal muscle arterioles. *Microcirculation* **19**: 327-335, 2012.

4. Al-Khazraji BK, Saleem A, Goldman D, Jackson DN. From one generation to the next: a comprehensive account of sympathetic receptor control in branching arteriolar trees. *J Physiol* **593**: 3093-3108, 2015.

5. Baker M, and Wayland, H. On-line volume flow rate and velocity profile measurement for blood in microvessels. *Microvascular Research* **7**: 131-143, 1974.

6. Bearden SE, Payne GW, Chisty A, Segal SS. Arteriolar network architecture and vasomotor function with ageing in mouse gluteus maximus muscle. *J Physiol* **561**: 535-545, 2004.

7. Bishop JJ, Nance, P.R., Popel, A.S., Intaglietta, M., and Johnson P.C. Relationship between erythrocyte aggregate size and flow rate in skeletal muscle venules. *Am J Physiol Heart Circ Physiol* **286**: H113-H120, 2004.

8. Boegehold MA. Shear-dependent release of venular nitric oxide: effect on arteriolar tone in rat striated muscle. *Am J Physiol* **271**: H387-H395, 1996.

9. Bohlen HG, Gore, R.W., and Hutchins, P.M. Comparison of microvascular pressures in normal and spontaneously hypertensive rats. *Microvascular Research* **13**: 125-130, 1977.

10. Bradbury S. The evolution of the microscope. In, edn: Pergamon, Oxford, 1967.

11. Chambers R, and Zweifach, B.W. Topography and function of mesenteric capillary circulation. *American Journal of Anatomy*: 173-200, 1944.

12. Das B, Bishop, J.J., Kim, S., Meiselman, H.J., Johnson P.C., and Popel, A.S. Red blood cell velocity profiles in skeletal muscle venules at low flow rates are described by the Casson model. *Clinical Hemorheology and Microcirculation* **36**: 217-233, 2007.

13. Davies PF. Flow-mediated endothelial mechanotransduction. *Physiol Rev* **75**: 519-560, 1995.

14. Ellsworth ML, Liu, A., Dawant, B., Popel, A.S., and Pittman, R.N. Analysis of vascular pattern and dimensions in arteriolar networks of the retractor muscle in young hamsters. *Microvascular Research* **34**: 168-183, 1987.

15. Engelson ET, Skalak, T.C., Schmid-Schonbein, G.W. The microvasculature in skeletal muscle I Arteriolar network in rat spinotrapezius muscle. *Microvascular Research* **30**: 29-44, 1985.

16. Faber JE. In situ analysis of alpha-adrenoceptors on arteriolar and venular smooth muscle in rat skeletal muscle microcirculation. *Circulation Research* **62**: 37-50, 1988.

17. Fahraeus R. The suspension stability of the blood. *Physiological Reviews* **9**: 241-274, 1929.

18. Fahraeus R, and Lindqvist, T. The viscosity of the blood in narrow capillary tubes. *American Journal of Physiology* **96**: 562-568, 1931.

19. Fishman AP, and Richards, D.W. Circulation of the blood, men and ideas. *Oxford Univ Press*, 1964.

20. Frasher Jr. WG, and Wayland, H. A repeating modular organization of the microcirculation of the cat mesentery. *Microvascular Research* **4**: 62-76, 1972.

21. Gaehtgens P. Why Networks? *International Journal of Microcirculation: Clinical and Experimental* **11**: 123-132, 1992.

22. Gauer OH. *Harvey: William Harvey, "Founders of Experimental Physiology"*edn1971.

23. Grant RT. Direct observation of skeletal muscle blood vessels (rat cremaster). *Journal of Physiology* **172**: 123-137, 1964.

24. Gross JF, Intaglietta, M., and Zweifach, B.W. Network model of pulsatile hemodynamics in the microcirculation of the rabbit omentum. *American Journal of Physiology* **226**: 1117-1123, 1974.

25. Henriche HN, and Hecke, A. A gracilis muscle preparation for quantitative microcirculatory studies in the rat. *Microvascular Research* **15**: 349-356, 1978.

26. Hoole S, and Van Leeuwenhoek, A. edn, vol. 11798.

27. Jackson DN, Milne KJ, Noble EG, Shoemaker JK. Gender-modulated endogenous baseline neuropeptide Y Y1-receptor activation in the hindlimb of Sprague-Dawley rats. *J Physiol* **562**: 285-294, 2005.

28. Jackson DN, Moore AW, Segal SS. Blunting of rapid onset vasodilatation and blood flow restriction in arterioles of exercising skeletal muscle with ageing in male mice. *J Physiol* **588**: 2269-2282, 2010.

29. Johnson PC. Introduction: Overview of the microcirculation. In: *Handbook of Physiology, Microcirculation*, 2nd edn: Elsevier inc., 2008, p. xi-xxiv.

30. Koller A, and Kaley, G. Endothelial regulation of wall shear stress and blood flow in skeletal muscle microcirculation. *Am J Physiol* **260**: H862-H868, 1991.

31. Krogh A. The anatomy and physiology of capillaries: Lecture I Introductory— The distribution and number of capillaries in selected organs. *Yale University Press*: 1-22, 1922.

32. Kuchan MJ, Jo, H., and Frangos, J.A. Role of G proteins in shear stress-mediated nitric oxide production by endothelial cells. *Am J Physiol* **267**: C753-C758, 1994.

33. Lee JS, and Duling, B.R. Role of flow dispersion in the computation of microvascular flows by the dual-slit method. *Microvascular Research* **37**: 280-288, 1989.

34. Lee JS, and Nellis, S. Modeling study on the distribution of flow and volume in the microcirculation of cat mesentery. *Annals of Biomedical Engineering* **2**: 206-216, 1974.

35. Ley K, Pries, A.R., and Gaehtgens, P. Topological structure of rat mesenteric microvessel networks. *Microvascular Research* **32**: 315-322, 1986.

36. Lipowsky HH, and Zweifach, B.W. Network analysis of microcirculation of cat mesentery. *Microvascular Research* **7**: 73-83, 1974.

37. Lipowsky HH, Kovalcheck, S., and Zweifach, B.W. The distribution of blood rheological parameters in the microvasculature of cat mesentery. *Circulation Research* **43**: 738-749, 1978.

38. Nakano A, Sugii, Y., Minamiyama, M., and Niimi, H. Measurement of red cell velocity in microvessels using particle image velocimetry (PIC). *Clinical Hemorheology and Microcirculation* **29**: 445-455, 2003.

39. Ortiz D, Briceno JC, Cabrales P. Microhemodynamic parameters quantification from intravital microscopy videos. *Physiol Meas* **35**: 351-367, 2014.

40. Pittman RN, and Ellsworth, M.L. Estimation of red cell flow in microvessels: Consequences of the Baker-Wayland spatial averaging model. *Microvascular Research* **32**: 371-388, 1986.

41. Pries AR, Ley, K., and Gaehtgens, P. Generalization of the Fahraeus principle for microvessel networks. *Am J Physiol Heart Circ Physiol* **251**: H1324-H1332, 1986.

42. Pries AR, Secomb, T.W., and Gaehtgens, P. Relationship between structural and hemodynamic heterogeneity in microvascular networks. *Am J Physiol Heart Circ Physiol* **270**: H545-H553, 1996.

43. Pries AR, Secomb, T.W., Gaehtgens, P., and Gross, J.F. Blood Flow in Microvascular Networks. *Circulation Research* **67**: 826-834, 1990.

44. Sato M, and Ohshima, N. Velocity profiles of blood flow in microvessels measured by ten channels' dual-sensor method. *Biorheology* **25**: 279-288, 1988.

45. Schmid-Schonbein GW, and Zweifach, B.W. RBC Velocity profiles in arterioles and venules of the rabbit omentum. *Microvascular Research* **10**: 153-164, 1975.

46. Schmid-Schonbein GW, Skalak, R., Usami, S., and Chien, S. Cell distribution in capillary networks. *Microvascular Research* **19**: 18-44, 1980.

47. Sriram K, Intaglietta M, Tartakovsky DM. Non-Newtonian flow of blood in arterioles: consequences for wall shear stress measurements. *Microcirculation* **21**: 628-639, 2014.

48. Strahler AN. Quantitative analysis of watershed geomorphology. *Transactions American Geophysical Union* **38**: 913-920, 1957.

49. Tangelder GJ, Slaaf, D.W., Arts, T., and Reneman, R.S. Wall shear rate in arterioles in vivo: least estimates from platelet velocity profiles. *Am J Physiol Heart Circ Physiol* **254**: H1059-H1064, 1988.

50. Tangelder GJ, Slaaf, D.W., Muijtjens, A.M.M., Arts, T., Oude Egbrink, M.G., and Reneman, R.S. Velocity profiles of blood platelets and red blood cells flowing in arterioles of the rabbit mesentery. *Circulation Research* **59**: 505-514, 1986.

51. Tangelder GJ, Teirlinck, H.C., Slaaf, D.W., and Reneman R.S. Distribution of blood platelets flowing in arterioles. *Am J Physiol* **248**: H318-H323, 1985.

52. VanTeeffelen JW, Segal SS. Rapid dilation of arterioles with single contraction of hamster skeletal muscle. *Am J Physiol Heart Circ Physiol* **290**: H119-127, 2006.

53. Weideman MP. Lengths and diameters of peripheral arterial vessels in the living animal. *Circulation Research* **10**: 686-690, 1962.

54. Wiedeman MP. Historical Introduction. In: *An introduction to microcirculation*: Academic Press, 1981, p. 3-11.

55. Zweifach BW. The structure and reactions of the small blood vessels in amphibia. *American Journal of Anatomy* **60**: 473-514, 1937.

56. Zweifach BW. The character and distribution of the blood capillaries. *The Anatomical Record* **73**: 475-495, 1939.

57. Zweifach BW, and Lipowsky, H.H. Quantitative studies of microcirculatory structure and function III Microvascular hemodynamics of cat mesentery and rabbit omentum. *Circulation Research* **41**: 380-390, 1977.

Chapter 2

Optimizing Arteriolar Network Hemodynamic Analysis Using an Integrated Model Derived from Experimental Data

2

2.1 Introduction

In skeletal muscle, the orchestration between competing vasoconstrictors and vasodilators is essential for precisely matching blood flow to metabolic rate. Acute changes in arteriolar network resistance are modulated through coordination of intrinsic (e.g., myogenic control and endothelium derived factors) and extrinsic (e.g., sympathetic nervous system; SNS) alterations in arteriolar diameter. The SNS provides potent vasoconstriction of arterioles through the release of norepinephrine (NE), adenosine triphosphate (ATP), and neuropeptide Y (NPY) that act on their associated receptors with varying potency, depending on the site of observation within the microvascular network [4]. In the face of ongoing vasoconstriction offered by the SNS, there are also a number of locally derived or released endothelial factors that evoke ongoing vasodilation at rest, as well as in response to increased metabolism [e.g., nitric oxide (NO), ATP, cyclooxygenase (COX), endothelial derived hyperpolarizing factor (EDHF), and adenosine from 5'-nucleotidase (5'NUC)] [8].

In the physics of viscous fluid flow, Poiseuille's law describes the inverse power relationship between tube diameter and resistance; in skeletal muscle microvascular networks, arterioles have the greatest capacity to constrict and dilate to alter flow resistance. Based on the high degree of regulation at the arteriolar level, studies of skeletal muscle microvascular regulation or dysregulation and rheology commonly employ point-source acquisition of arteriolar radius at one or more bifurcations using IVVM or from experiments using pressurized isolated microvessels. Although data from such studies have shaped our understanding of microvascular control, they limit our ability to accurately predict blood rheology in microvascular networks using theoretical modeling.

For decades, theoreticians and computational modelers have stressed that quantitative analysis of the distribution of microvascular blood flow and hematocrit requires a detailed description of the vascular network geometry [10]. In fact, hemodynamic characteristics of heterogeneous microvascular networks can only be adequately

described if both topological and geometric variability in network structure are considered [19]. As such, we have spent over 6 years developing and validating novel experimental tools and approaches to accurately measure: 1) arteriolar blood flow [3], 2) arteriolar network wall shear rates [2], 3) microvascular network geometry *in situ* [1]. By using an iterative approach, whereby our experiments promote the evolution of our theoretical model, several interesting and novel rheological phenomena have organically emerged. In order to utilize complex and heterogeneous experimentally derived microvascular network data for accurate theoretical modeling, one must not only match available data but must also consider more general network hemodynamic properties. Two of these properties that we believe are of particular importance are: 1) the overall pressure drop across the network (which informs us that network resistance is accurate), and 2) the Murray's Law exponent (which informs us that network structure and flow distribution are accurate).

Fundamentally, Murray's Law is a demonstration of network efficiency and describes the power relationship between the flow of a fluid (e.g., the blood) and the diameter of conduits within which the fluid is flowing (e.g., the arteriolar network of interest). Murray's Law is a mathematical description of this relationship, where an exponent of 3 is considered ideal in terms of efficiency. If, experimentally, our arteriolar networks obey a version of Murray's law, then the assumption is that the network is optimized for efficiency, and this property should be maintained by our computational model of blood flow in networks reconstructed from experimental data.

In the current study we address the impact of including variable capillary resistance and measured venular network geometry, as well as the resistance of small arterioles and venules, on the integrated accuracy of our computational model of network hemodynamics, including agreement with: 1) Murray's Law, and 2) well-established values for pressure drops across microvascular networks in skeletal muscle. The purpose of this work was to develop an approach to computational modeling of hemodynamics in large arteriolar-venular networks that permits accurate calculation of total blood flow (or, equivalently, overall resistance), blood flow distribution, and RBC distribution using geometric data that can be obtained *in vivo* during a relatively short observation time

(~several minutes). This ability to connect geometry to flow will make it possible to study microvascular regulation over a wide range of scales (~10 micrometers to several centimeters) and gain novel understanding of how intrinsic and extrinsic factors are integrated by the network to control blood flow to terminal arterioles. Our hypotheses are, 1) that both capillary resistance and venular network structure are important in determining the hemodynamics properties of microvascular networks, and 2) that by supplementing measured arteriolar network structure with measured venular network structure, estimated capillary resistance, and estimated resistance of unobserved small arterioles and venules, we will be able to accurately predict network hemodynamics.

2.2 Methods and Materials

2.2.1 Experimental Data Acquisition

Previously acquired intravital videomicroscopy (IVVM) images of the gluteus maximus (GM) muscle of n=8 male Sprague-Dawley rats (aged 8-9 weeks; 303 ± 15g) were used in this study. A detailed account of the complete experimental preparation and imaging method can be found in Al Tarhuni et al., 2016 [1]. The experimental procedure involved scanning complete arteriolar networks arising from the inferior gluteal artery in the left GM under baseline conditions. The rat GM preparation was developed in our lab and is the model choice for skeletal muscle hemodynamic studies due to its planar geometry and uniform thinness, which allow imaging access to the entire microcirculation, including the corresponding venular network, within a single focal plane. Therefore, the *in situ* imaging data were used to obtain geometrical and topological measurements on both arteriolar and venular networks.

The IVVM images were registered in Matlab (MathWorks Inc., Natick, MA, USA) to create a complete photomontage of the arteriolar and venular network. Quantitative reconstruction of each microvascular network involved placing nodes approximately 150 μm apart along unbranched segments. Each network was traced with nodes (given x-y coordinates) and cylindrical sub-segments that connect the nodes (Figure 18). The diameter and lengths of sub-segments were measured using ImageJ (NIH, Bethesda, MD,

USA) and input into a data file that stored the coordinate, node connectivity (topological) and geometrical (segment lengths and diameters) information.

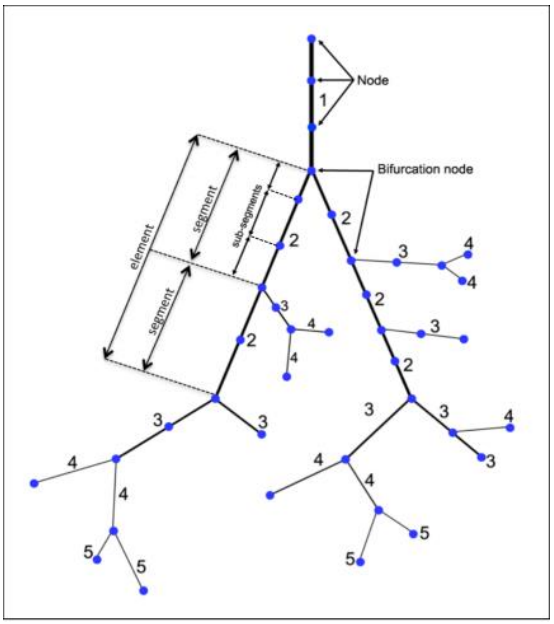

Figure 18: Schematic of node-segment representation in a simplified arteriolar network. Arteriolar networks were discretized into cylindrical sub-segments connected through nodes. Sub-segments connected serially in between two bifurcation nodes are termed a segment. A number of segments connected serially within the same topological order are termed an element [1].

The data was then fed through a centrifugal ordering algorithm in Matlab to generate arterioles and venules with orders ranging from 1st to 9th order for arterioles, and 1st to 11th for venules. The centrifugal algorithm assigned the main feed arteriolar or main draining venule an order of 1 and assigned higher order to daughter vessels that have diameters less than 80% of the parent and/or bifurcation angles greater than 15%.

Previous work in our group [1] reconstructed only arteriolar networks and obtained their overall geometric properties, such as diameter and length as a function of order. Below, we used the IVVM data from these same networks both to reconstruct the venular networks and obtain their overall geometric properties, including length and diameter ratios between vessels in successive orders.

2.2.2 Arteriole-Venule Connection

Following network reconstruction of arterioles and venules, the two components could be connected to create one complete network. In order to do this, the arteriolar outflow nodes were connected to venular inflow nodes with connecting segments (assuming a 1:1 ratio) by matching the terminal ends based on a target distance of 800 μm. The target distance of 800 μm was obtained from trial and error and the assumption that capillary beds are approximately 400 μm in length [9]. The target distance of 800 μm had minimal effect on total arteriolar flow (at 800 μm, the CV of total terminal arteriolar flow was smaller than at 300 μm or 500 μm). The matching algorithm was developed to pair terminal ends by minimizing the total error between the target distance and matched distance over all connecting segments. We assumed a ratio of 1:1 between terminal arteriolar and collecting venular segments as a start for our matching algorithm. Therefore, we ensured that the number of collecting venules registered was the same as those registered previously for terminal arterioles [1]. Once the two networks were connected, the segments between the terminal ends were assigned a set length and were used to include resistance of missing terminal segments and estimated capillary resistance (see below).

2.2.3 Resistance for Missing Terminal Vessels

From preliminary analyses of arteriolar and venular networks, we found that pressure curves from simulated data show a pressure drop that is smaller than expected. We hypothesized that the relatively small pressure drop could be due to missing resistances from terminal vessels that are likely not captured in the acquired data. In order to account for the resistance of missing terminal vessels, additional generations of virtual vessels were constructed for boundary segments between diameters of 9 μm and 50 μm in arteriolar networks, and 25 μm and 50 μm in venular networks, using measured diameter R_D, length R_L, and bifurcation R_B ratios [1]. R_D, R_L, and R_B are the ratios of the diameter, length, and number of vessels at any given order to the diameter, length, and number of vessels at the next highest order. These ratios are known as Horton's Laws, and they state that the diameter, length and number of vessels are related to topological order through a power-law relationship. By plotting the logarithm of diameter, length, and

number of vessels as a function of order, a linear relationship is obtained. Applying a linear regression analysis produces a line with a slope, which is used to calculate the ratios. Given the diameter and length of a terminal vessel segment, Horton's Laws could be used to calculate the diameter and length of the next generations of daughter vessels. The collection of diameters and lengths were input into Poiseuille's Law to calculate the total resistance of the missing generations (assuming symmetric bifurcations) for that terminal segment.

Poiseuille's Law:

$$Q = \frac{\Delta P\, r^4 \pi}{8\eta L},$$

where ΔP is pressure drop, r is radius, L is length, and η is viscosity, gives $\Re = \frac{8\eta L}{r^4 \pi}$, where $\Re$ is resistance. The resistance for the missing generations was calculated using Poiseuille's law, and the calculated resistance was added to each connecting segment using its diameter, given the set length and calculated resistance. To simplify the method, viscosity was assumed the same in all missing vessels and in the connecting segment.

2.2.4 Variable Capillary Resistance

A complete microvascular network requires all components that contribute to the overall network, including capillaries. In our current study, we were representing capillaries in each network by an estimated capillary resistance that was applied to the connecting segments between the arterioles and corresponding venules. Total capillary resistance was calculated based on an estimated pressure drop of 7 mmHg across rat skeletal muscle capillaries [12] and calibrated for each network's total input flow. Given known total input flow at first order arteriole and pressure drop across arterioles, the total resistance across capillaries could be calculated according to the following expressions:

$$\frac{\Re_{Capillaries}}{\Re_{Arterioles}} = \frac{\Delta P_{Capillaries}}{\Delta P_{Arterioles}}$$

Rearrange to get: $\Re_{Capillaries} = \frac{\Delta P_{Capillaries}}{\Delta P_{Arterioles}} \times \Re_{Arterioles}$

$$\Re_{Capillaries} = \frac{\Delta P_{Capillaries}}{\Delta P_{Arterioles}} \times \frac{\Delta P_{Arterioles}}{Total\ Flow}$$

Therefore, $\Re_{Capillaries} = \frac{\Delta P_{Capillaries}}{Total\ Flow}$

Total input blood flow for each network at first order arteriole was calculated using the power-law equation developed by Al-Khazraji et al. [3]: $Blood\ Flow = 10^{-3.43} x\ Diameter^{2.63}$. Total capillary resistance was then distributed to each connecting vessel, either uniformly (*constant capillary resistance*) or based on its diameter (*variable capillary resistance*). Since capillary bed resistances are approximately in parallel, having N terminal arterioles means each added resistance is $N\Re_{Capillaries}$ for the constant resistance case. For the variable resistance case, power law dependence on TA diameter was assumed ($\Re \sim 1/D^n$, $n>0$) so that resistance added to the i^{th} connecting segment is

$$\Re_i(D_i) = \frac{\sum_{j=1}^{N} D_j^n}{D_i^n} \Re_{Capillaries}$$

Our choice for exponent *n* was based on trial and error. We varied exponent n, compared its effects on Murray's Law exponent, and chose the exponent that minimized the error in Murray's Law. On average, at n=4.5, Murray's law exponent was closest to 3 for all eight arteriolar networks. For further details please see **Appendix A**, where we present a comparison of Murray's law exponent obtained when we use constant capillary resistance, variable capillary resistance with exponent n=3, and variable capillary with exponent n=4.5.

2.2.5 Two-phase Blood Flow Model

After the geometrical and topological parameters of the complete networks were measured, they were input into our two-phase (RBC and plasma) steady state blood flow

model to calculate flow rate across the network components. The flow model, adapted from Pries et al. [20,21] predicts the distribution of total blood flow and hematocrit (and therefore, viscosity) at every segment in the network by an iterative method, which solves for blood flow and hematocrit alternately until the values converge. Boundary conditions that specify known (or estimated) inflow and outflow values of blood flow or pressure (ΔP fixed at 80 mmHg) are required. Inlet hematocrit (fixed at 0.419) is also set in the model. The procedure begins with calculation of blood flow in each segment. Blood flow in each segment and pressure at each node is calculated by solving a system of linear equations that describe mass balance in blood flow and RBC flow at every bifurcation.

$$\sum_i Q_{ij} = 0,$$

$$\sum_i H_{D_{ij}} Q_{ij} = 0,$$

where ij denotes a vessel segment connecting nodes i and j. Blood flow in each segment is given by the following:

$$Q_{ij} = \frac{(p_i - p_j)}{r_{ij}}$$

where $p_i - p_j$ is the pressure drop between nodes i and j, and r_{ij} is the flow resistance in the vessel segment, as described by Poiseuille's Law:

$$r_{ij} = \frac{8\eta L}{\pi R^4}$$

where η is the apparent blood viscosity, and L and R are the length and radius of the segment, respectively.

Using results from the previous step and known rheological properties of blood, the second part of the procedure can be carried out to solve hematocrit and viscosity in each vessel segment. In addition to RBC mass conservation, to calculate discharge hematocrit (H_D), the phase separation effect, which describes the disproportionate distribution of

RBC and plasma at diverging bifurcations, is applied. Apparent viscosity in each segment is then computed from an empirical relation based on the Fahraeus-Lindqvist effect, which states that viscosity changes as a (non-linear) function of hematocrit and vessel diameter. A second empirical relation (developed by Pries et al. in 1990 [20]) based on the Fahraeus effect is used to estimate tube hematocrit (H_T), which is given as a function of discharge hematocrit and vessel diameter. The Fahraeus effect states that tube hematocrit decreases with a decrease in vessel size.

Following computation of hematocrit and viscosity, the procedures are repeated with newly calculated viscosity as inputs for flow and pressure measurements in the first step, and continue until values converge (error tolerance set at 10^{-11}).

2.2.6 Validation with Streak Length Method

The streak length method is an experimental method based on measuring average velocity of red blood cells and area of vessel in which they flow: $Q = V_{mean} \times Area_{Vessel}$. RBC streaks are formed on images of fluorescent RBCs that are taken at 5-20 ms exposure times. Velocity of RBCs can be calculated from the distance travelled (streak length – RBC length) over the exposure time. The mean velocity is calculated from the maximum velocity (centerline streak velocity) over the velocity ratio (given as a function of diameter) [3]. Our streak length measurements were performed in an arteriolar network, which we refer to as the validation network, at 15 different segments of 5 bifurcations. Mass conservation was tested at each bifurcation by comparing flow in parent and daughter vessels.

2.2.7 Validation with Murray's Law

Our interests in blood flow distribution require an additional validation step. In addition to validating predicted flow values, we also consider the behaviour or efficiency of flow in vessels, which can be tested through Murray's Law. Murray's law describes the power-law dependence of blood flow on diameter, stating that the optimal arteriolar network structure is obtained when blood flow is $\propto$ diameter^3. At exponent 3, the metabolic and cardiac work required to maintain blood flow in arterioles is minimized.

Murray's law is a power relation, therefore, plotting blood flow (nL/s) over diameter (μm) on a log-log scale gives a scatter plot that follows a linear pattern. Applying linear regression, we could model the pattern with a line, the slope of which is the Murray's law exponent of interest.

2.2.8 Statistical Analysis

Statistical analysis was performed in Prism (version 7.0d, GraphPad Software Inc., La Jolla, CA, USA). In the validation of our model, Linear Regression was applied to flow data to evaluate the correlation between predicted values and measured values. Linear Regression was also applied to log-log plots of flow over diameter to assess the extent to which our model obeys Murray's Law. The slope of the regression line gives Murray's Law exponent. To assess changes in variability in the distribution of blood flow and tube hematocrit at terminal arterioles between different network components, coefficient of variation (CV) values were presented as mean ± SEM. One-way ANOVA with Tukey's multiple comparisons was applied to evaluate significance between network component groups.

2.3 Results

2.3.1 Network Approach for Arteriolar Blood Flow Analysis

Figure 19 shows a complete photomontage of 1 out of the 8 rat GM microvascular networks analyzed in this study. The photomontage was analyzed in Matlab to register coordinates of nodes (150 μm apart) in both the arteriolar and venular networks, giving rise to thousands of segments between nodes across each network. Lumen diameter was measured in ImageJ at and assigned to each segment.

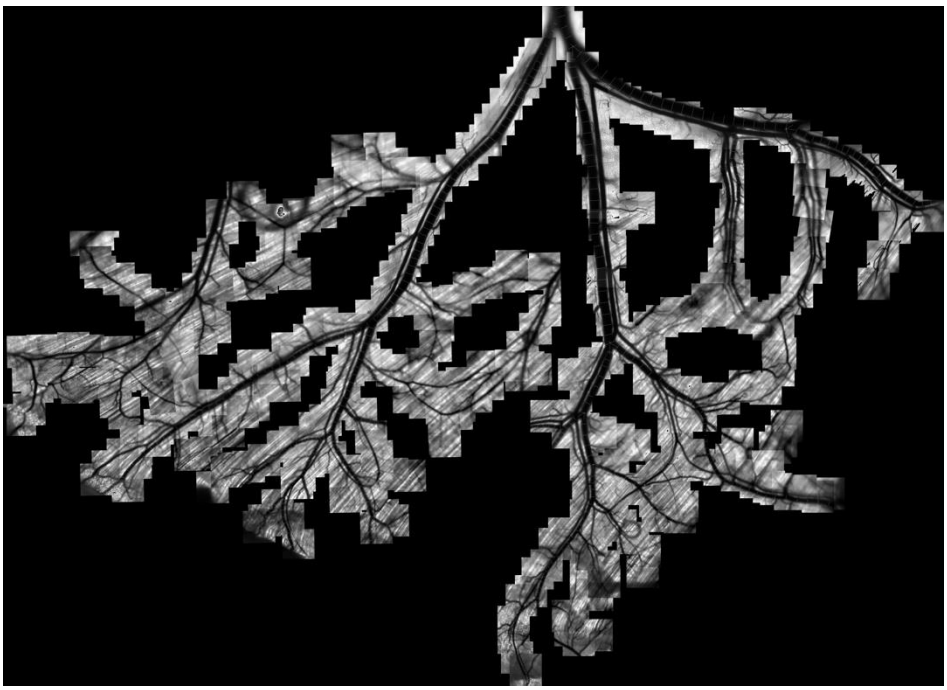

Figure 19: Photomontage of a microvascular network imaged with IVVM in the rat gluteus maximus muscle.

Each arteriolar network, followed by the corresponding venular network, was reconstructed in Matlab from the registered coordinates to create skeleton structures. The arteriolar and venular networks were then input into a matching algorithm that allows their terminal ends to be paired based on an 800 μm target distance. Figure 20 shows the reconstructed arteriolar (red) and venular (blue) networks with segments (dotted) connecting their terminal ends for a complete microvascular network.

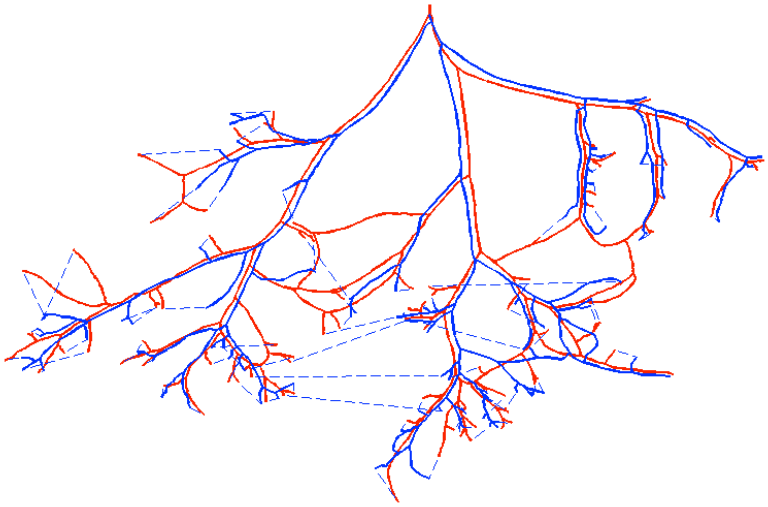

Figure 20: Network reconstruction of arteriolar (red) and venular (blue) network. Segment connections made between terminal arteriolar nodes and collecting venular nodes.

Note that as part of this network reconstruction, we obtained for the first time in the GM complete venular network structures as well as their overall geometric properties. The dependence of vessel diameter and length on venular order (starting from the largest venular which is paired with the feeding arteriole) are shown in Figures 21 and 22, respectively. By analyzing this data, we obtained a diameter ratio, R_D, of 1.2481 and a length ratio, R_L, of 1.3257 between successive generations, similar to values for the arteriolar network obtained in [1].

Interestingly, loops or arcades were observed in arterioles and venules of all 8 networks analyzed in this study. In our geometric analyses, all loops were systematically cut for applying our ordering algorithm, which currently does not process loops. However, for flow simulations, all loops were intact to provide a more accurate representation of flow through the networks.

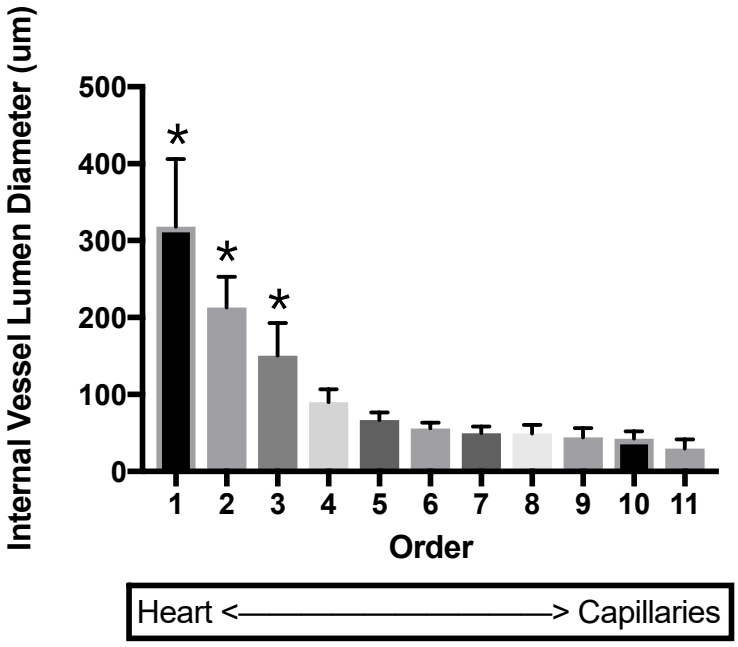

Figure 21: Relationship between mean luminal diameter and order. Data presented as mean ± SEM (n=8 animals). (* Significantly different from subsequent order at $p < 0.005$).

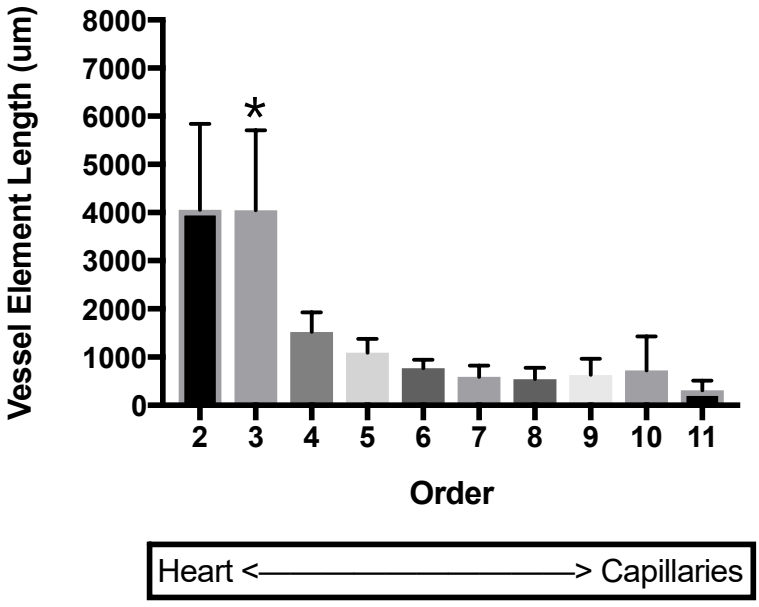

Figure 22: Relationship between vessel element length and order. Data presented as mean ± SEM (n=8 animals). (* Significantly different from subsequent order at $p < 0.005$).

When we input the networks into our steady state model and simulated flow and pressure across all nodes, we noticed that the pressure drop across each complete network was smaller than expected for a normal network. We hypothesized that the small pressure drop was likely due to missing terminal segments that were not visible in the photomontage, which would account for an amount of resistance. To test our hypothesis, we calculated resistance with diameters and lengths of missing vessel segments (for each arteriolar and venular network) from geometric ratios. Geometric ratios describe the relationship between parent and daughter's geometric properties. Therefore, the calculated additional resistances depend on the size and length of each "terminal" arteriolar or venular segment, and were assigned to the connecting segment between the arterioles and venules. The resulting simulation with the added missing resistances gave rise to a pressure drop (mean ΔP = 58.67 mmHg for n=8 network) that was closer to an expected normal pressure drop, with an average increase of 85% over all 8 networks. A pressure drop from the network in Figures 19 and 20 is shown in Figure 23. Vessel segment pressures (mmHg) calculated from blood flow simulations in the complete network were plotted. Arteriolar segments are shown in red and venular segments in blue.

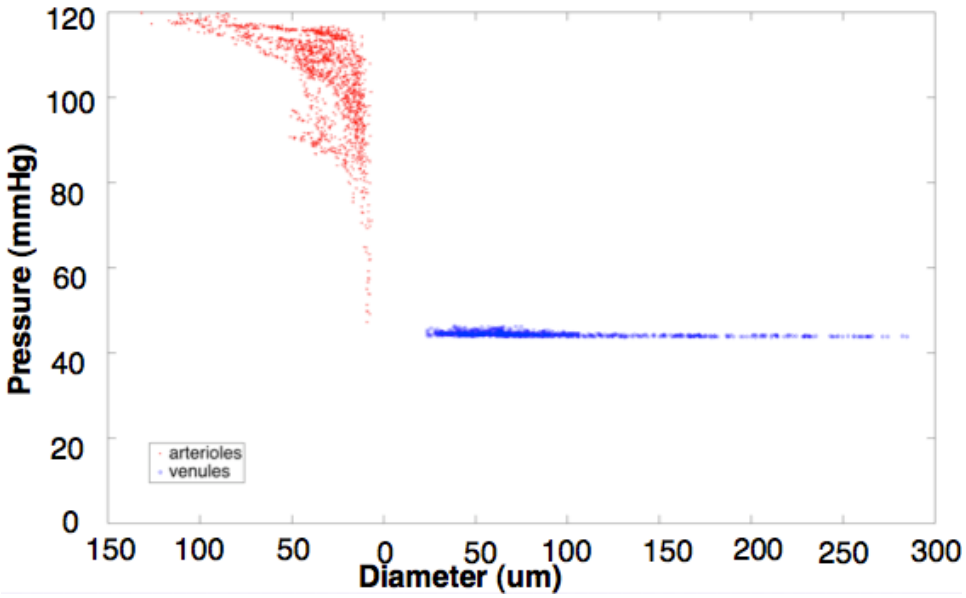

Figure 23: Vessel segment pressures (mmHg) calculated from blood flow simulations in the complete network. Arteriolar segments were plotted in red and

venular segments in blue. Inlet pressure was fixed at 120 mmHg for all 8 networks. Average venular pressure drop was 7.61 mmHg.

From the pressure drop, we were able to estimate the total capillary resistance for each network based on an estimated pressure drop of 7 mmHg across the capillaries, and known resistance and pressure drop across arterioles. Total capillary resistance was then distributed to each terminal arteriole, based on its diameter to produce variable resistance between capillary segments. The effect of capillary resistance and venular network geometry on flow and RBC distribution in terminal segments of arterioles was then explored. Specifically, we studied the effects of adding capillary resistance and corresponding venular network geometry on the mean overall arteriolar resistance (calculated as $\frac{\Delta P_{Arterioles}}{Total\ Flow}$), the coefficient of variation (CV) of flow distribution in terminal arterioles, and the CV of tube hematocrit in terminal arterioles (Figure 24). We found that capillary resistance caused a significant increase in mean overall resistance across the network, whereas the venular network did not significantly change the mean overall resistance. Interestingly, when we focus on flow distribution or tube hematocrit distribution individually, we see the individual effects of capillary resistance and venules on arterioles. When we added only capillary resistance to the terminal arterioles, the CV of both flow distribution and tube hematocrit at the terminal arterioles was significantly increased. When we added the corresponding venular network to the arterioles plus capillary resistance, the CV of flow distribution at the terminal arterioles did not significantly change, whereas the CV of tube hematocrit was significantly reduced relative to arterioles plus capillary resistance alone (Figure 24).

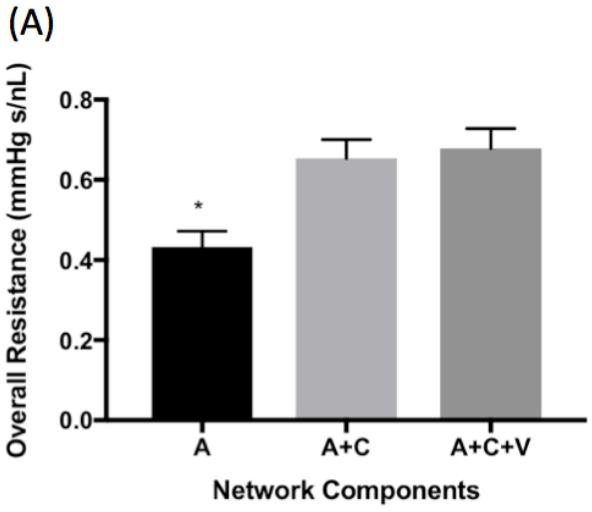

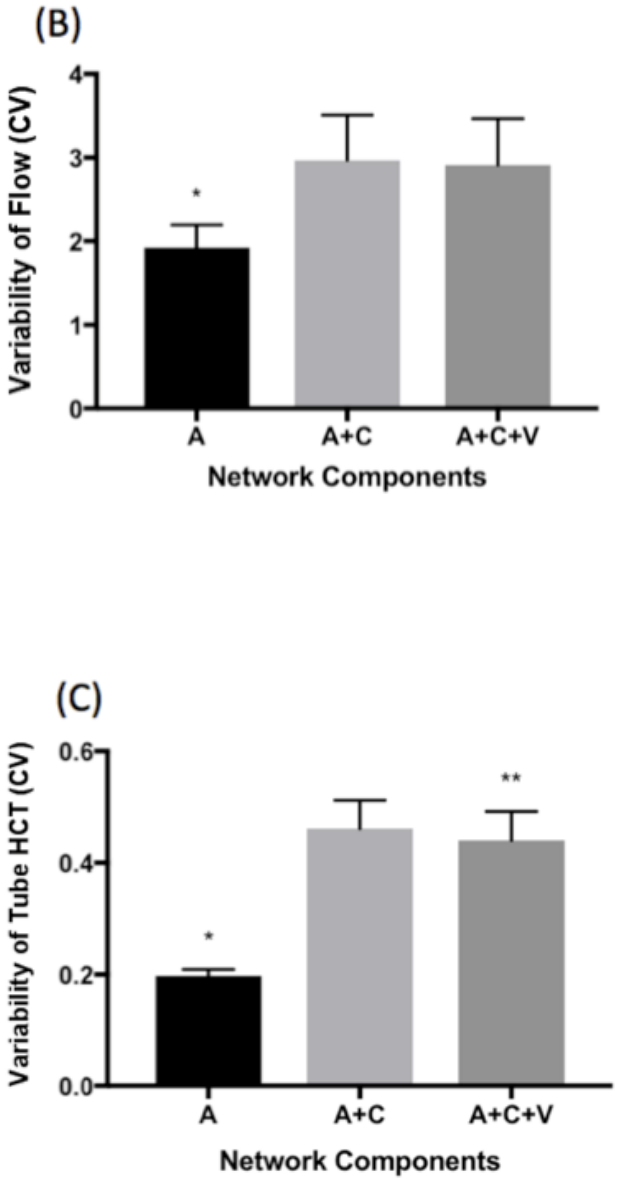

Figure 24: Effect of adding capillary resistance and corresponding venular network geometry on (A) mean overall resistance, (B) coefficient of variation (CV) of flow in terminal arterioles, and (C) CV of tube hematocrit in terminal arterioles. Change in variables are shown with respect to network components: A arterioles alone, A+C arterioles plus capillary resistance, A+C+V arterioles plus capillary resistance and venular network geometry. Data are expressed as mean ± SEM after one-way ANOVA with Tukey's multiple comparisons, n=8 networks per group. (Figure **A**: *significantly different from all subsequent groups at $p < 0.0001$; Figure **B**: *significantly different

from all subsequent groups at $p < 0.03$; Figure **C**: *significantly different from all subsequent groups at $p < 0.004$, **significantly different from previous group at $p < 0.03$).

2.3.2 Network Analysis Technique Validation

After we demonstrated the importance of capillary resistance for flow simulations, the next step was to validate the simulated arteriolar flow values (with added variable capillary resistance) using measured flow. We measured flow using the streak length method, which is based on measuring centerline velocity of red blood cells and area of vessel in which they flow. The method involved capturing streaks of fluorescently labeled RBCs from images taken at 5-20 ms exposure times. Velocity of RBCs could be calculated from the distance travelled (streak length – RBC length) over the exposure time. The mean blood velocity was a simple ratio of the maximum RBC velocity (centerline streak velocity) over the velocity ratio (given as a function of diameter). The final result gave blood flow via $Q = V_{mean} \times Area$. Further details on the streak length method can be found in Al Khazraji et al. [3].

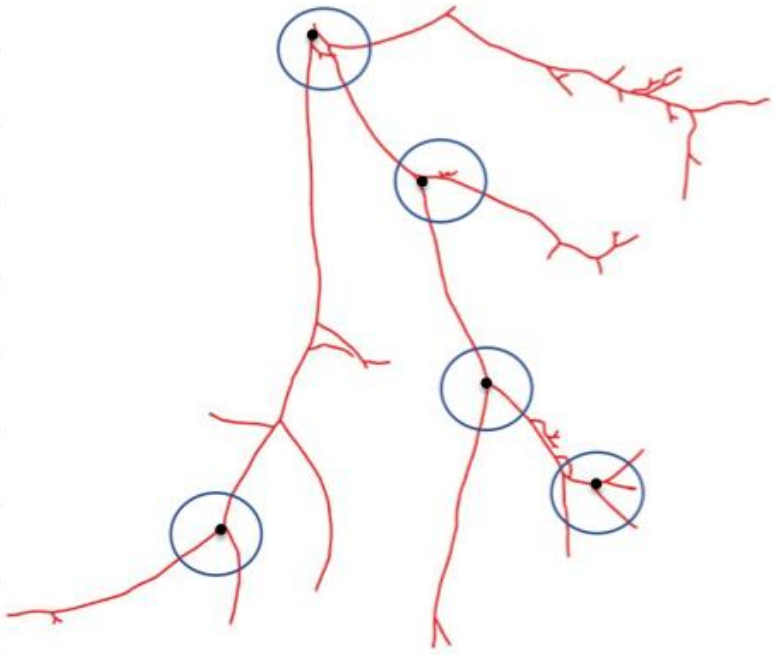

Figure 25: Reconstructed arteriolar network for validation. Flow was measured using the streak length method in 15 vessel segments making up the 5 bifurcations, indicated in blue circles. Black dots represent the intersection between vessels of the bifurcations analyzed for flow.

Measured flow was obtained at 15 segments in a rat GM arteriolar network (Figure 25), which we refer to as the validation network (different from the 8 networks previously mentioned). Following the same model as above with the added variable capillary resistance, the predicted flow (nL/s) through the arteriolar network was compared to the measured flow (nL/s) at the 15 measurement segments (Figure 26). Our predicted results show close agreement to the measured results with an error of less than 33%, calculated as an average error over the 15 segments.

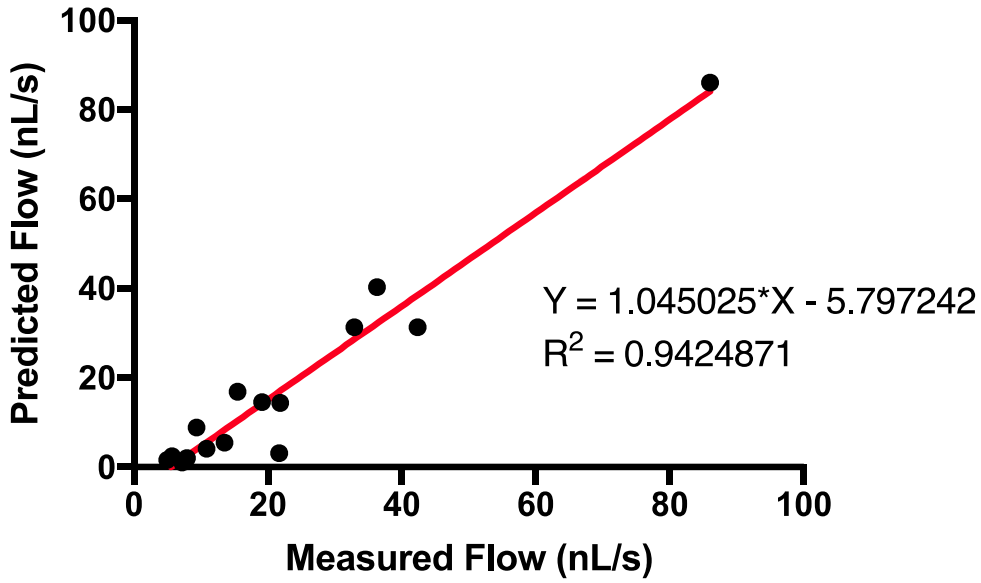

Figure 26: Validating predicted flow (nL/s) using model vs. measured flow (nL/s) using the streak length method. Flow in the validation network was simulated through arterioles (with added capillary resistance) and measured in 15 arteriolar vessel segments of the same network.

Our second validation step involved the Murray's law exponent, which is a power-law dependence of blood flow on diameter, stating that the optimal arteriolar network structure is obtained when **blood flow is $\propto$ diameter^3**. We were able to show that our model predicts blood flow within a 33% error; however, this previous experiment does not tell us whether the diameter dependence of blood flow through vessels is correct. A normal functioning network will obey Murray's law such that blood will flow most efficiently through vessels when the power law relationship between blood flow and diameter is given by the power law relation (as above), where the exponent is 3.

To start, Murray's law exponent was explored in measured data from our validation network. Figure 27 shows the 15 flow measurements plotted over diameter on a log-log scale. The slope of the log-log line was the Murray's law exponent, which we found to be approximately 2.90. Comparing this exponent to 3, we could see that our validation

network did indeed obey a form of Murray's law, and therefore could be used as a reference for our 8 networks, through which we simulated flow in our model.

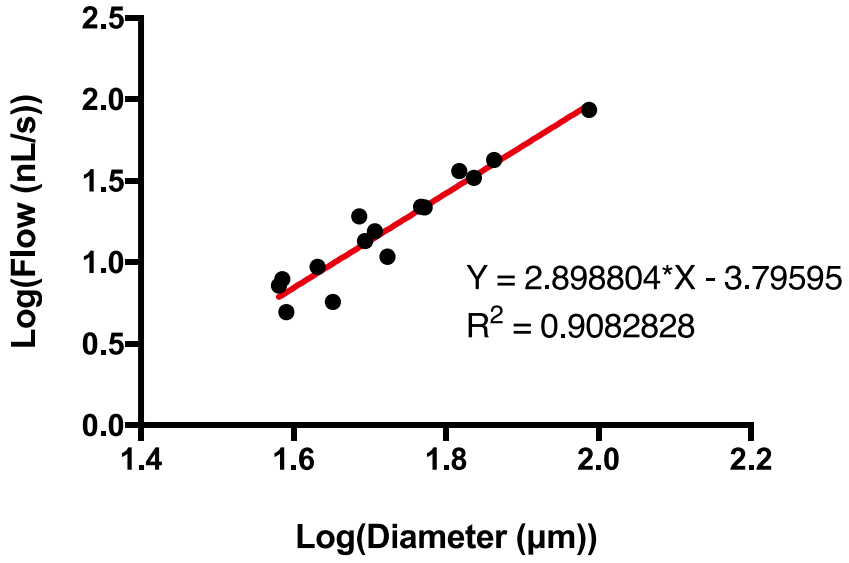

Figure 27: Validation with Murray's law exponent and measured flow. Log-log of measured flow (nL/s) vs. diameter (µm) show a strong linear correlation. Flow was experimentally measured using SLM (streak length method) in 15 vessel segments. Log-log plot of flow vs. diameter produced for validation of Murray's Law exponent, given by slope of log-log line.

We added variable capillary resistance and the corresponding venular network to the terminal segments of each arteriolar network (n=8) before applying our flow model, and plotted flow in every segment of each network (1000s total) over the corresponding segment diameters on a log-log scale to get 8 Murray's Law relations (Figure 28). The Murray's law exponents obtained from these 8 networks and their pooled result are presented in Table 1. The Murray's law exponent obtained from pooled data was 2.78 and is within 5% of the experimentally measured exponent of 2.90 that we obtained from the validation network. Therefore, our model for blood flow using added variable capillary resistance also closely obeyed the form of Murray's laws found in arteriolar networks of the rat GM.

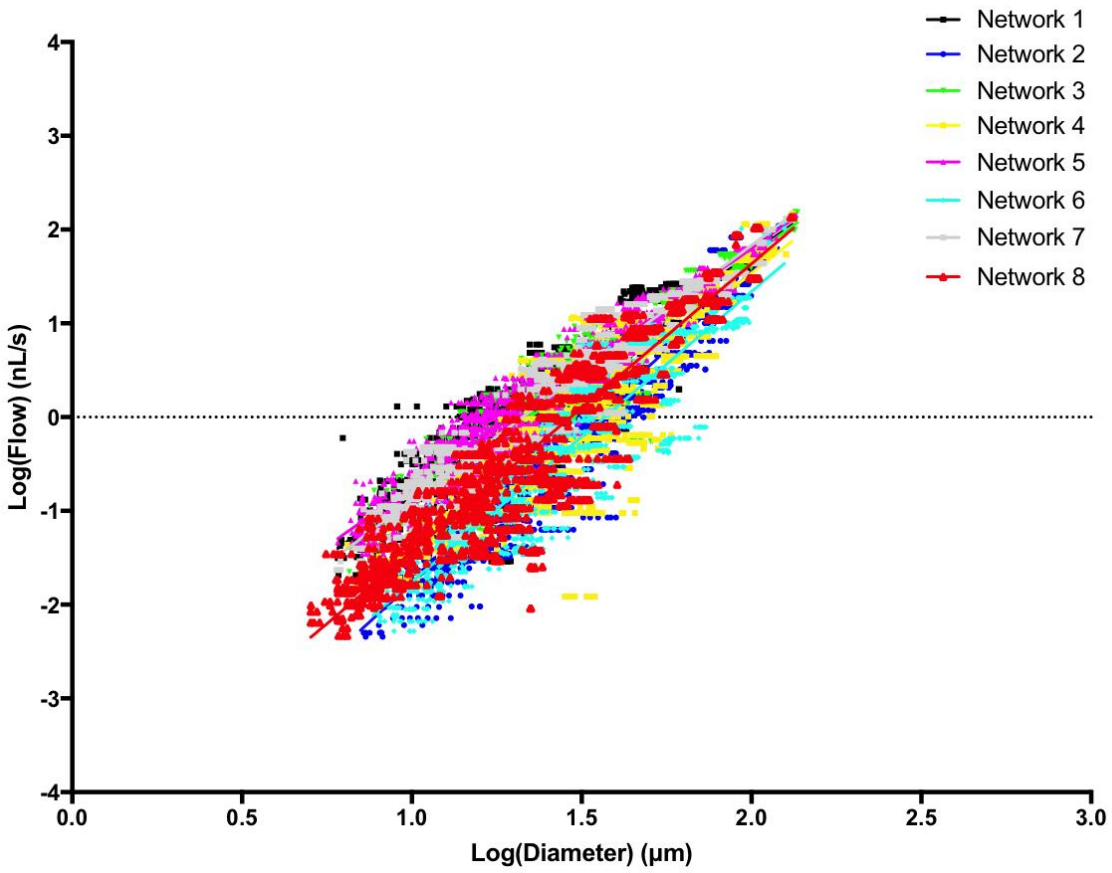

Figure 28: Log-log plots of predicted blood flow and arteriolar diameter show a strong linear correlation for n=8 networks. Linear Regression fits: $R^2 > 0.75$, $p < 0.0001$. The slopes of the linear regression lines ranged from 2.540 to 3.316, with a mean ± SD of 2.853 ± 0.28. Data from all networks were also pooled into one plot to give a slope of 2.778 ($R^2 = 0.765$, $p < 0.0001$).

Table 1: Murray's law validation for predicted flow in n=8 networks. Predicted flow (nL/s) in complete network structures of arterioles, capillary resistance, and venules gave an average Murray's Law exponent for arterioles of 2.78.

Network	Linear Regression Equation	R^2	95% Confidence Interval of Slope
1	log(Q) = 2.581*log(D) – 3.417	0.83	2.522 to 2.640
2	log(Q) = 3.316*log(D) – 5.088	0.88	3.258 to 3.375
3	log(Q) = 2.636*log(D) – 3.553	0.84	2.573 to 2.700
4	log(Q) = 2.862*log(D) – 4.190	0.77	2.786 to 2.938
5	log(Q) = 2.540*log(D) – 3.280	0.91	2.501 to 2.579
6	log(Q) = 3.096*log(D) – 4.854	0.85	3.033 to 3.159
7	log(Q) = 2.718*log(D) – 3.603	0.91	2.668 to 2.768
8	log(Q) = 3.071*log(D) – 4.506	0.87	3.014 to 3.127
Pooled	**log(Q) = 2.778*log(D) – 3.970**	**0.77**	**2.750 to 2.805**

2.4 Discussion

The purpose of this work was to develop an approach to computational modeling of hemodynamics in large arteriolar-venular networks that permits accurate calculation of total blood flow, blood flow distribution, and RBC distribution using geometric data obtained in vivo. Based on the concept that microvascular structure strongly influences hemodynamic behavior, and our two-phase flow model, which considers disproportionate distribution of RBCs and plasma at diverging bifurcations (phase separation effect), we

hypothesized that capillary resistance and venular network structure are necessary parameters to consider when modeling the hemodynamic or rheological properties of arteriolar networks.

2.4.1 Integration of Variable Capillary Resistance

Herein we are first to report that if capillaries are not considered, overall arteriolar resistance is underestimated. We also report that the variability of flow distribution at terminal arterioles is underestimated. Our data show that when the GM arteriolar network resistance is estimated without considering the integration of capillary resistance and venular network inputs, our model underestimated resistance by at least 50% (Figure 24). Until now, there have been no reports showing similar correlations or the effects of capillary resistance on arteriolar resistance or RBC distribution in the rat GM. The integration of variable capillary resistance normalized the arteriolar pressure drop to values commonly reported [7] and significantly increased the efficiency of arteriolar network flow (as indicated by Murray's Exponent; Table 1). RBC distribution at arteriolar bifurcations (as indicated by CV of tube hematocrit: Figure 24) also increased with the integration of capillary resistance. Variable capillary resistance at terminal arterioles was applied such that low flow terminal segments receive higher resistance (based on their relatively smaller diameter), and high flow terminal segments receive lower resistance (based on their relatively larger diameter). Therefore, our results were consistent with our technique for integrating capillary resistance.

2.4.2 Integration of Venular Network Structure

We are first to also report that if venules are not considered, the variability of RBC distribution at terminal arterioles is overestimated with respect to arterioles plus capillaries. Our data show that when the CV of tube hematocrit in the GM arteriolar network was estimated with capillary resistance and without the integration of venular network inputs, our model overestimates CV of tube hematocrit by 5% (Figure 24). Interestingly, blood flow at arteriolar bifurcations (as indicated by CV of blood flow: Figure 24) was unaffected by the integration of venular network geometry.

2.4.3 Our Network Approach

Our approach began by considering pressure drops across networks. After reconstructing a complete arteriolar-venular network structure, we applied our two-phase flow model and calculated the pressure drop across the network for known total flow (calculated from relation given in [3]). We found that the pressure drop was lower than expected for a complete skeletal muscle network [7,16]. Our hypothesis was that, although *in vivo* networks were acquired across a large range of orders (1 to 9), the total network resistance was not captured due to missing terminal segments, which contribute to total resistance. To account for this, we calculated resistance of missing vessel segments for each arteriolar and venular network, using measured geometric ratios [1], and calculated pressure drop from our simulations. The results showed that with our approach of adding missing resistance, our network model presents more realistic pressure drops from flow simulations.

Our next step assessed the effects of capillary resistance and venular network geometry on overall resistance, blood flow and hematocrit distribution in arterioles. Arterioles are a major site of blood flow regulation, mostly due to their ability to control resistance, and therefore, have been a focus in most hemodynamic studies of microvascular networks [2,6,13,22-25]. Our network acquisition *in vivo* ensures that we are capturing true structural and functional information [1,3,5], as they appear in normal physiological conditions, that is to say they are intact physiologically and all signals and pathways are functioning. Furthermore, when acquiring network data, we tried to capture as much of the network structure as possible; however, terminal vessels that are deeper in tissue were more difficult to capture at a given focal depth. We have seen that the two-phase hemodynamic model used in our study can predict hemodynamic parameters across *in vivo* networks; however, it is limited by the microvascular structure that is provided to it. For example, the effects of missing terminal vessels on resistance and pressure can be substantial, as described above. Therefore, we proposed that we must expect a change in predicted hemodynamics in arteriolar networks when we include capillary resistance and venular network geometry. The effects we found were indeed appreciable and demonstrate the need to incorporate complete network geometry in hemodynamic

analyses that use current mathematical models. Previous studies that include similar models worked in the rat mesentery [15], or rabbit omentum and human conjunctiva [11]. Until now, capillary resistance and venular networks were not considered in arteriolar hemodynamic analyses of rat GM.

We validated our complete network approach using flow measurements from streak data and Murray's Law. Strong correlations ($R^2 = 0.94$) between predicted and measured flow data were found for one validation network (Figure 26). Murray's Law exponent of 2.90 for measured flow data also showed that our validation network obeyed Murray's Law (Figure 27). We compared Murray's law exponent obtained from our predicted flow data (in arterioles with capillary resistance and corresponding venular network) for n=8 networks (Table 1; Figure 28) to 2.90 obtained from our measured flow data in n=1 validation arteriolar network. Although Murray's Law has been employed before, for example to assess the condition of vascular bifurcations in coronary arteriolar blood vessels in pigs [14], quantify vascular branching geometry in blue crabs [18], or analyze structure and hemodynamics of vascular networks in chicken chorioallantoic membrane [17], it has not been used to assess a hemodynamic model for GM arteriolar networks.

2.4.4 Limitations

Although the purpose of our study was to develop an approach using complete *in vivo* geometric data, our focus in terms of structure was only on arteriolar and venular networks. Due to the dearth of studies on venules, we were interested in isolating the effects of venular network geometry on arteriolar network hemodynamics, while considering the effects of capillaries in terms of their resistance alone. The effects of capillary structure were, therefore, not included in this study.

In addition to estimating capillary resistance, we also estimated resistance of missing terminal arterioles and collecting venules. To calculate resistance, we used geometric ratios, which generate a single diameter and length for both daughter vessels to a parent vessel with known diameter and length. Although this method provided a sufficient estimation of missing resistance, it did not account for the asymmetric nature of microvascular vessels. By assigning the same diameter and length to both daughter

vessels, the algorithm using geometric ratios assumed that the missing vessels are symmetric. Future analyses on asymmetries could be performed and applied at every order on the relative diameter and lengths between daughter vessels.

2.5 Conclusion

We have provided a novel technique for accurately analyzing arteriolar hemodynamics that involved a network-oriented approach including capillary resistance and venular network geometry. We showed that blood flow and RBC distribution in arterioles depend on the presence of capillaries and venules, and also tested the validity of our technique using measured blood flow and Murray's Law, which rated the accuracy of our model predictions. Herein, the tools developed in our study could be used in future studies to analyze network hemodynamics in rat GM muscles under different conditions.

2.6 References

1. Al Tarhuni M, Goldman D, Jackson DN. Comprehensive In Situ Analysis of Arteriolar Network Geometry and Topology in Rat Gluteus Maximus Muscle. *Microcirculation* **23**: 456-467, 2016.

2. Al-Khazraji BK, Jackson DN, Goldman D. A Microvascular Wall Shear Rate Function Derived From In Vivo Hemodynamic and Geometric Parameters in Continuously Branching Arterioles. *Microcirculation* **23**: 311-319, 2016.

3. Al-Khazraji BK, Novielli NM, Goldman D, Medeiros PJ, Jackson DN. A simple "streak length method" for quantifying and characterizing red blood cell velocity profiles and blood flow in rat skeletal muscle arterioles. *Microcirculation* **19**: 327-335, 2012.

4. Al-Khazraji BK, Saleem A, Goldman D, Jackson DN. From one generation to the next: a comprehensive account of sympathetic receptor control in branching arteriolar trees. *J Physiol* **593**: 3093-3108, 2015.

5. Bearden SE, Payne GW, Chisty A, Segal SS. Arteriolar network architecture and vasomotor function with ageing in mouse gluteus maximus muscle. *J Physiol* **561**: 535-545, 2004.

6. Boegehold MA. Shear-dependent release of venular nitric oxide: effect on arteriolar tone in rat striated muscle. *Am J Physiol* **271**: H387-H395, 1996.

7. Bohlen HG, Gore, R.W., and Hutchins, P.M. Comparison of microvascular pressures in normal and spontaneously hypertensive rats. *Microvascular Research* **13**: 125-130, 1977.

8. Duza T, and Sarelius, I.H. Conducted dilations intitiated by purines in arterioles are endothelium dependent and require endothelial Ca2+. *Am J Physiol Heart Circ Physiol* **285**: H26-H37, 2003.

9. Ellis CG, Bateman, R.M., Sharpe, M.D., Sibbald, W.J., and Gill, R. Effect of a maldistribution of micrvascular blood flow on capillary 02 extraction in sepsis. *Am J Physiol Heart Circ Physiol* **282**: H156-H164, 2002.

10. Ellsworth ML, Liu, A., Dawant, B., Popel, A.S., and Pittman, R.N. Analysis of vascular pattern and dimensions in arteriolar networks of the retractor muscle in young hamsters. *Microvascular Research* **34**: 168-183, 1987.

11. Fenton BM, and Zweifach, B.W. Microcirculatory model relating geometrical variation to changes in pressure and flow rate. *Annals of Biomedical Engineering* **9**: 303-321, 1981.

12. Fronek K, and Zweifach, B.W. Microvascular pressure distribution in skeletal muscle and the effect of vasodilation. *American Journal of Physiology* **228**: 791-796, 1975.

13. Jackson DN, Moore AW, Segal SS. Blunting of rapid onset vasodilatation and blood flow restriction in arterioles of exercising skeletal muscle with ageing in male mice. *J Physiol* **588**: 2269-2282, 2010.

14. Kassab GS, and Fung, Y.B. The pattern of coronary arteriolar bifrucations and the uniform shear hypothesis. *Annals of Biomedical Engineering* **23**: 13-20, 1995.

15. Ley K, Pries, A.R., and Gaehtgens, P. Topological structure of rat mesenteric microvessel networks. *Microvascular Research* **32**: 315-322, 1986.

16. Lipowsky HH, and Zweifach, B.W. Network Analysis of Microcirculation of Cat Mesentery. *Microvascular Research* **7**: 73-83, 1974.

17. Maibier M, Reglin B, Nitzsche B, Xiang W, Rong WW, Hoffmann B, Djonov V, Secomb TW, Pries AR. Structure and hemodynamics of vascular networks in the chorioallantoic membrane of the chicken. *Am J Physiol Heart Circ Physiol* **311**: H913-H926, 2016.

18. Marcinek D, and LaBarbera, M. Quantitative branching geometry of the vascular system of the blue crab, Callinectes sapidus (Arthropoda, Crustacea): A test of Murray's law in an open circulatory system. *Biol Bull* **186**: 124-133, 1994.

19. Pries AR, Secomb, T.W., and Gaehtgens, P. Relationship between structural and hemodynamic heterogeneity in microvascular networks. *Am J Physiol Heart Circ Physiol* **270**: H545-H553, 1996.

20. Pries AR, Secomb, T.W., Gaehtgens, P., and Gross, J.F. Blood Flow in Microvascular Networks. *Circulation Research* **67**: 826-834, 1990.

21. Pries AR, Secomb, T.W., Gebner, T., Sperandio, M.B., Gross, J.F., and Gaehtgens, P. Resistance to Blood Flow in Microvessels in Vivo. *Circulation Research* **75**: 904-915, 1994.

22. Sriram K, Intaglietta M, Tartakovsky DM. Non-Newtonian flow of blood in arterioles: consequences for wall shear stress measurements. *Microcirculation* **21**: 628-639, 2014.

23. Tangelder GJ, Slaaf, D.W., Arts, T., and Reneman, R.S. Wall shear rate in arterioles in vivo: least estimates from platelet velocity profiles. *Am J Physiol Heart Circ Physiol* **254**: H1059-H1064, 1988.

24. Tangelder GJ, Slaaf, D.W., Muijtjens, A.M.M., Arts, T., Oude Egbrink, M.G., and Reneman, R.S. Velocity profiles of blood platelets and red blood cells flowing in arterioles of the rabbit mesentery. *Circulation Research* **59**: 505-514, 1986.

25. Tangelder GJ, Teirlinck, H.C., Slaaf, D.W., and Reneman R.S. Distribution of blood platelets flowing in arterioles. *Am J Physiol* **248**: H318-H323, 1985.

Chapter 3

General Discussion

3

3.1 Contributions

This thesis presented a true network approach based on *in situ* vascular data from a live animal for accurately studying network hemodynamics in the rat GM. Novel techniques that integrate capillaries and venules were provided for accurate arteriolar hemodynamic analyses, such as blood flow and RBC distribution. The estimation errors in flow and RBC distribution that were revealed when arterioles are studied alone reinforce the need and purpose of network-oriented analysis.

Building on the network concept that has been the foundation of many studies, our thesis is the first to evaluate the complete microvascular network hemodynamics [1,4,6,9-11]. Our thesis builds upon these previous studies that evaluate network hemodynamics [9-11], through our unique approach for capturing most microcirculatory vessels (not previously acquired) using both geometrical and theoretical tools.

With the rat GM preparation, we were able to capture both arteriolar and venular network structure (geometrical and topological) in a single acquisition experiment. Our preference for the rat GM preparation stems from its relevant function in locomotion, its common presence in both sexes of all mammalian species, and its uniform thinness that (in combination with the intrinsic anatomical layout of the microvasculature within the GM) allows for complete network imaging at a single focal plane. Our tools for reconstructing the topological structures and for measuring geometrical parameters were applied to both arterioles and venules. With our network structural information as inputs, our two-phase steady state theoretical blood flow model could be used to generate hemodynamic results and provide insight into structural and functional accuracy of our GM network of interest. By integrating tools with known established physical principles, it became readily apparent that we were unable to capture all vessels in the complete microvascular network. It was from our calculation of resistance and pressure, which was found to be different from known or expected values [3], that we suspected the case of missing terminal vessels that are not visible in IVVM images. To address this

challenge, we estimated missing vessels (and their resistances) using geometric ratios that describe the relation between parent and daughter vessels in terms of their diameter (R_D), length (R_L) and number of vessels (R_B) at a given order (also known as Horton's Laws). Integrating theoretical methods has enabled us to correct for our inability to capture every single vessel in the network. This supports the value of considering theoretical physical principles when describing physiological blood flow and rheological phenomena, as they exist *in vivo*.

With the integration of experimental methods (such as IVVM and the rat GM preparation) and theoretical tools (such as the two-phase steady blood flow model, and theoretical estimation of missing terminal segments) we were also able to isolate and quantify the effects of integrating components of the microcirculation (arterioles, capillaries and venules). Specifically, we quantified the effects of capillary resistance and venular network geometry on overall arteriolar resistance, and blood flow and tube hematocrit distribution at terminal arterioles. We reported that if the nature of variable capillary resistance was not considered, overall arteriolar resistance was underestimated, and consequently, the variability of flow distribution at terminal arterioles was also underestimated. Furthermore, we are first to also report that if venular network structure was not integrated or considered, the variability of RBC distribution at terminal arterioles was underestimated with respect to arterioles alone and overestimated with respect to arterioles plus capillary resistance.

We validated the efficiency of our network using Murray's Law, and the accuracy of our network using measured blood flow. Murray's Law is a calculation of network efficiency and describes the power relationship between the flow of blood and diameter of the arteriolar network of interest, where blood flow is $\propto$ diameter^3. At exponent 3, the metabolic and cardiac work required to maintain blood flow in arterioles is minimized. We validated the accuracy of our new model for arteriolar hemodynamic analysis with experimental measurements of arteriolar blood flow using the streak length method [2]. Strong correlations ($R^2 = 0.94$) between predicted and measured flow data were found for one validation network (*Chapter 2*, Figure 26). We obtained Murray's law exponent from our predicted flow data for n=8 networks (*Chapter 2*; Table 1, Figure 28), which we

compared to Murray's law exponent obtained from measured results (*Chapter 2*, Figure 27). Although Murray's Law has been employed before in other microvascular beds [5,7,8], we are the first to use it to assess a hemodynamic model for GM arteriolar networks.

Overall, this thesis culminates 8 years of work in our lab. By integrating all our techniques, it becomes obvious that in order to move forward in understanding blood flow and RBC distribution at bifurcations, a comprehensive analysis as presented in this thesis is required. We demonstrated that it is necessary to consider at least capillaries and venules in arteriolar hemodynamic analyses.

3.2 Future Work

One technique missing from our current work is RBC flow measurement, which would provide crucial data for understanding regulation of blood flow and oxygen delivery, and could be used to further validate our network hemodynamic model. We have an idea on how to approach this using fluorescent RBCs and the streaks used to measure blood flow. We are currently in the process of completing this work to the point where it can be published and used in future experimental and modeling studies.

In the future, we will also work to understand how capillary structure will alter hemodynamic behaviour to further drive our understanding of 4-dimensional modeling of rheological properties. In addition, our hemodynamic analyses techniques have been developed such that, given any network, we can accurately predict flow and hematocrit throughout the network, and further relate hemodynamic results to measures of structure. Specifically, one could study intra-network variability of flow or hematocrit at all levels of the complete network (not only at terminal vessels) from arterioles to venules, and compare results to what has been studied experimentally [3].

Furthermore, our model could be applied to other networks from rats under different conditions, such as hypertensive, diabetic, or obese rats, to investigate the effects of these conditions on microcirculatory structure and function.

3.3 References

1. Al Tarhuni M, Goldman D, Jackson DN. Comprehensive In Situ Analysis of Arteriolar Network Geometry and Topology in Rat Gluteus Maximus Muscle. *Microcirculation* **23**: 456-467, 2016.

2. Al-Khazraji BK, Novielli NM, Goldman D, Medeiros PJ, Jackson DN. A simple "streak length method" for quantifying and characterizing red blood cell velocity profiles and blood flow in rat skeletal muscle arterioles. *Microcirculation* **19**: 327-335, 2012.

3. Bohlen HG, Gore, R.W., and Hutchins, P.M. Comparison of microvascular pressures in normal and spontaneously hypertensive rats. *Microvascular Research* **13**: 125-130, 1977.

4. Ellsworth ML, Liu, A., Dawant, B., Popel, A.S., and Pittman, R.N. Analysis of vascular pattern and dimensions in arteriolar networks of the retractor muscle in young hamsters. *Microvascular Research* **34**: 168-183, 1987.

5. Kassab GS, and Fung, Y.B. The pattern of coronary arteriolar bifrucations and the uniform shear hypothesis. *Annals of Biomedical Engineering* **23**: 13-20, 1995.

6. Ley K, Pries, A.R., and Gaehtgens, P. Topological structure of rat mesenteric microvessel networks. *Microvascular Research* **32**: 315-322, 1986.

7. Maibier M, Reglin B, Nitzsche B, Xiang W, Rong WW, Hoffmann B, Djonov V, Secomb TW, Pries AR. Structure and hemodynamics of vascular networks in the chorioallantoic membrane of the chicken. *Am J Physiol Heart Circ Physiol* **311**: H913-H926, 2016.

8. Marcinek D, and LaBarbera, M. Quantitative branching geometry of the vascular system of the blue crab, Callinectes sapidus (Arthropoda, Crustacea): A test of Murray's law in an open circulatory system. *Biol Bull* **186**: 124-133, 1994.

9. Pries AR, Secomb, T.W., and Gaehtgens, P. Relationship between structural and hemodynamic heterogeneity in microvascular networks. *Am J Physiol Heart Circ Physiol* **270**: H545-H553, 1996.

10. Pries AR, Secomb, T.W., Gaehtgens, P., and Gross, J.F. Blood Flow in Microvascular Networks. *Circulation Research* **67**: 826-834, 1990.

11. Zweifach BW, and Lipowsky, H.H. Quantitative studies of microcirculatory structure and function III Microvascular hemodynamics of cat mesentery and rabbit omentum. *Circulation Research* **41**: 380-390, 1977.

Appendix A: Capillary Resistance

In our study, we were representing capillaries in each network by an estimated capillary resistance that was applied to the connecting segments between the arterioles and corresponding venules. Total capillary resistance was calculated based on an estimated pressure drop of 7 mmHg across rat skeletal muscle capillaries and calibrated for each network's total input flow. Given known total input flow at first order arteriole and pressure drop across arterioles, the total resistance across capillaries could be calculated according to the following expressions:

$$\frac{\Re_{Capillaries}}{\Re_{Arterioles}} = \frac{\Delta P_{Capillaries}}{\Delta P_{Arterioles}}$$

Rearrange to get: $\Re_{Capillaries} = \frac{\Delta P_{Capillaries}}{\Delta P_{Arterioles}} \times \Re_{Arterioles}$

$$\Re_{Capillaries} = \frac{\Delta P_{Capillaries}}{\Delta P_{Arterioles}} \times \frac{\Delta P_{Arterioles}}{Total\ Flow}$$

Therefore, $\Re_{Capillaries} = \frac{\Delta P_{Capillaries}}{Total\ Flow}$

Total input blood flow for each network at first order arteriole was calculated using the power-law equation: Blood Flow = $10^{-3.43}$xDiameter$^{2.63}$. Total capillary resistance was then distributed to each connecting vessel, either uniformly (*constant capillary resistance*) or based on its diameter (*variable capillary resistance*). Since capillary bed resistances are approximately in parallel, having N terminal arterioles means each added resistance is $N\Re_{Capillaries}$ for the constant resistance case. For the variable resistance case, power law dependence on TA diameter was assumed ($\Re \sim 1/D^n$, $n>0$) so that resistance added to the i^{th} connecting segment is

$$\Re_i(D_i) = \frac{\sum_{j=1}^{N} D_j^n}{D_i^n} \Re_{Capillaries}$$

Our choice for exponent n was based on trial and error. We varied exponent n, compared its effects on Murray's Law exponent, and chose the exponent that minimized the error in Murray's Law. On average, at n=4.5, Murray's law exponent was closest to 3 for all 8 arteriolar networks. Here we present the results found for Murray's law exponent under different applications of capillary resistance in 1 rat GM network.

Using our model and added constant capillary resistance, we obtained a Murray's law exponent of 2.197 and an R^2 = 0.83 (Figure 1). Using variable capillary resistance and exponent n=3, we obtained a Murray's law exponent of 2.231 and R^2 = 0.83 (Figure 2). When we change exponent n to 4.5, we obtained a Murray's law exponent of 2.619 and R^2 = 0.85 (Figure 3).

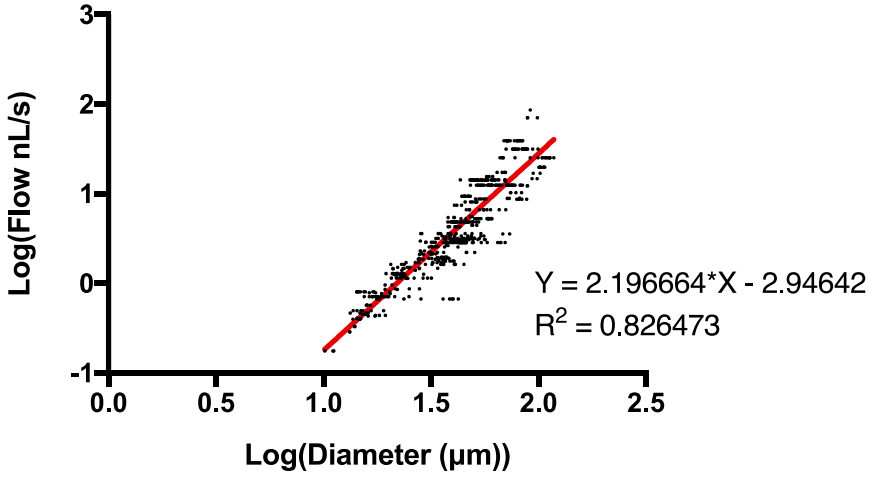

Figure 1: Log-log plot of predicted flow (nL/s) in arterioles with added *constant* capillary resistance versus arteriolar diameter (µm).

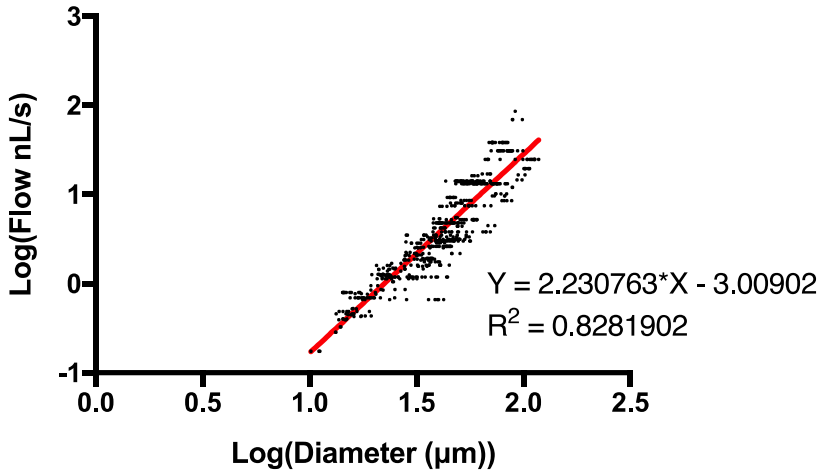

Figure 2: Log-log plot of predicted flow (nL/s) in arterioles with added *variable* capillary resistance using exponent **n=3** versus arteriolar diameter (µm).

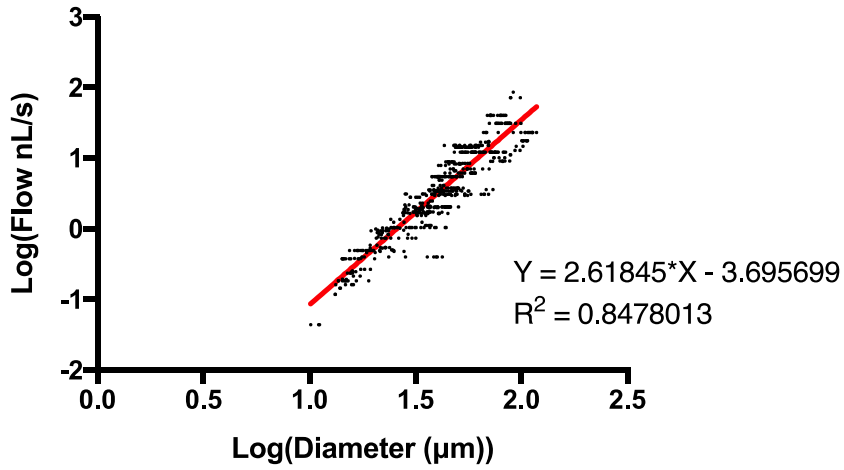

Figure 3: Log-log plot of predicted flow (nL/s) in arterioles with added *variable* capillary resistance using exponent **n=4.5** versus arteriolar diameter (µm).

We also compared our results to those obtained for arterioles alone using the Fry approach [1]. The Fry approach is a blood flow estimation method that does not require complete boundary data, and operates using a least-squares error minimization for given target pressure and shear stress values. When we apply the Fry method to the same arteriolar network, we obtained a Murray's law of 2.698 and $R^2 = 0.82$ (Figure 4).

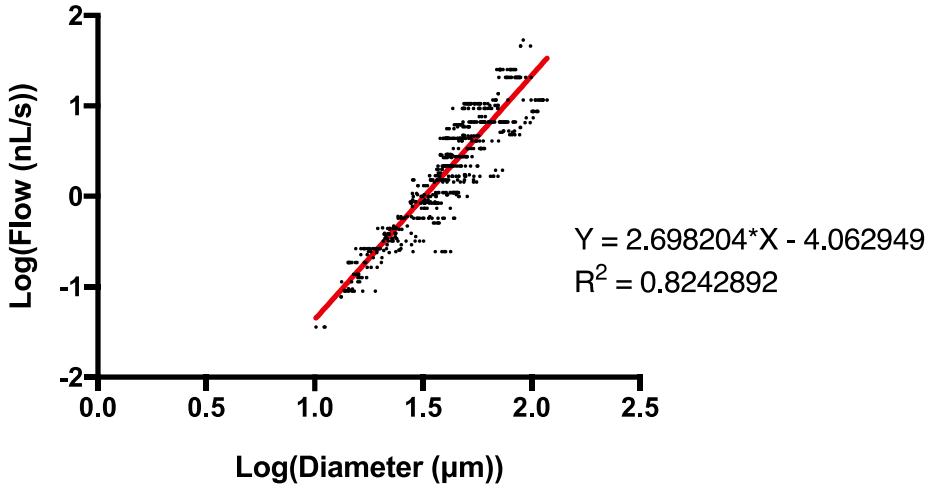

Figure 4: Log-log plot of predicted flow (nL/s) in arterioles using the Fry approach versus arteriolar diameter (µm).

Based on our desire to optimize R^2 for Murray's law and get close to the measured Murray's law exponent of 2.9 (*Chapter 2*: Figure 27), our method using variable capillary resistance with exponent n=4.5 provided approximately the best value, and was definitely better than our method using constant capillary resistance. Using variable capillary resistance with n=4.5, our Murray's law exponent was comparable to that obtained using the Fry method, but did slightly better in terms of R^2. Furthermore, the Fry method requires the asummption of a target shear stress value and does not benefit from incorporation of additional physiological data (such as venular network structure and small vessel resistance), and so is less suitable for the type of detailed network analysis that we are pursuing.

References:

1. Farid Z, Saleem AH, Al-Khazraji BK, Jackson DN, Goldman D. Estimating blood flow in skeletal muscle arteriolar trees reconstructed form in vivo data using the Fry approach. *Microcirculation*. 2017; **24**: e12378.

Appendix B: Figure Permissions

Copyright Clearance Center RightsLink®

Home | Account Info | Help

Title: Network analysis of microcirculation of cat mesentery
Author: H.H. Lipowsky,B.W. Zweifach
Publication: Microvascular Research
Publisher: Elsevier
Date: January 1974

Logged in as:
Zahra Farid
Account #:
3001327403
LOGOUT

Order Completed

Thank you for your order.

This Agreement between Ms. Zahra Farid ("You") and Elsevier ("Elsevier") consists of your license details and the terms and conditions provided by Elsevier and Copyright Clearance Center.

Your confirmation email will contain your order number for future reference.

printable details

License Number	4417860978120
License date	Aug 28, 2018
Licensed Content Publisher	Elsevier
Licensed Content Publication	Microvascular Research
Licensed Content Title	Network analysis of microcirculation of cat mesentery
Licensed Content Author	H.H. Lipowsky,B.W. Zweifach
Licensed Content Date	Jan 1, 1974
Licensed Content Volume	7
Licensed Content Issue	1
Licensed Content Pages	11
Type of Use	reuse in a thesis/dissertation
Portion	figures/tables/illustrations
Number of figures/tables/illustrations	1
Format	electronic
Are you the author of this Elsevier article?	No
Will you be translating?	No
Original figure numbers	Figure 3.
Title of your thesis/dissertation	Optimizing arteriolar network analysis using an integrated hemodynamic model derived from experimental data
Expected completion date	Aug 2018
Estimated size (number of pages)	90

Title: A repeating modular organization of the microcirculation of cat mesentery

Author: Wallace G. Frasher,Harold Wayland

Publication: Microvascular Research

Publisher: Elsevier

Date: January 1972

Order Completed

Thank you for your order.

This Agreement between Ms. Zahra Farid ("You") and Elsevier ("Elsevier") consists of your license details and the terms and conditions provided by Elsevier and Copyright Clearance Center.

Your confirmation email will contain your order number for future reference.

printable details

License Number	4417861198675
License date	Aug 28, 2018
Licensed Content Publisher	Elsevier
Licensed Content Publication	Microvascular Research
Licensed Content Title	A repeating modular organization of the microcirculation of cat mesentery
Licensed Content Author	Wallace G. Frasher,Harold Wayland
Licensed Content Date	Jan 1, 1972
Licensed Content Volume	4
Licensed Content Issue	1
Licensed Content Pages	15
Type of Use	reuse in a thesis/dissertation
Portion	figures/tables/illustrations
Number of figures/tables/illustrations	1
Format	electronic
Are you the author of this Elsevier article?	No
Will you be translating?	No
Original figure numbers	Figure 3.
Title of your thesis/dissertation	Optimizing arteriolar network analysis using an integrated hemodynamic model derived from experimental data
Expected completion date	Aug 2018

Title: Comparison of microvascular pressures in normal and spontaneously hypertensive rats

Author: H.Glenn Bohlen,Robert W. Gore,Phillip M. Hutchins

Publication: Microvascular Research

Publisher: Elsevier

Date: January 1977

Order Completed

Thank you for your order.

This Agreement between Ms. Zahra Farid ("You") and Elsevier ("Elsevier") consists of your license details and the terms and conditions provided by Elsevier and Copyright Clearance Center.

Your confirmation email will contain your order number for future reference.

printable details

License Number	4417960151140
License date	Aug 28, 2018
Licensed Content Publisher	Elsevier
Licensed Content Publication	Microvascular Research
Licensed Content Title	Comparison of microvascular pressures in normal and spontaneously hypertensive rats
Licensed Content Author	H.Glenn Bohlen,Robert W. Gore,Phillip M. Hutchins
Licensed Content Date	Jan 1, 1977
Licensed Content Volume	13
Licensed Content Issue	1
Licensed Content Pages	6
Type of Use	reuse in a thesis/dissertation
Portion	figures/tables/illustrations
Number of figures/tables/illustrations	1
Format	electronic
Are you the author of this Elsevier article?	No
Will you be translating?	No
Original figure numbers	Figure 1.
Title of your thesis/dissertation	Optimizing arteriolar network analysis using an integrated hemodynamic model derived from experimental data
Expected completion date	Aug 2018
Estimated size (number	90

Title: A gracilis muscle preparation for quantitative microcirculatory studies in the rat

Author: Herman N. Henrich,Agnes Hecke

Publication: Microvascular Research

Publisher: Elsevier

Date: May 1978

Order Completed

Thank you for your order.

This Agreement between Ms. Zahra Farid ("You") and Elsevier ("Elsevier") consists of your license details and the terms and conditions provided by Elsevier and Copyright Clearance Center.

Your confirmation email will contain your order number for future reference.

printable details

License Number	4417960313103
License date	Aug 28, 2018
Licensed Content Publisher	Elsevier
Licensed Content Publication	Microvascular Research
Licensed Content Title	A gracilis muscle preparation for quantitative microcirculatory studies in the rat
Licensed Content Author	Herman N. Henrich,Agnes Hecke
Licensed Content Date	May 1, 1978
Licensed Content Volume	15
Licensed Content Issue	3
Licensed Content Pages	8
Type of Use	reuse in a thesis/dissertation
Portion	figures/tables/illustrations
Number of figures/tables/illustrations	1
Format	electronic
Are you the author of this Elsevier article?	No
Will you be translating?	No
Original figure numbers	Figure 2.
Title of your thesis/dissertation	Optimizing arteriolar network analysis using an integrated hemodynamic model derived from experimental data
Expected completion date	Aug 2018
Estimated size (number of pages)	90

Title: Cell distribution in capillary networks

Author: G.W. Schmid-Schönbein,R. Skalak,S. Usami,S. Chien

Publication: Microvascular Research

Publisher: Elsevier

Date: January 1980

Order Completed

Thank you for your order.

This Agreement between Ms. Zahra Farid ("You") and Elsevier ("Elsevier") consists of your license details and the terms and conditions provided by Elsevier and Copyright Clearance Center.

Your confirmation email will contain your order number for future reference.

printable details

License Number	4417960757385
License date	Aug 28, 2018
Licensed Content Publisher	Elsevier
Licensed Content Publication	Microvascular Research
Licensed Content Title	Cell distribution in capillary networks
Licensed Content Author	G.W. Schmid-Schönbein,R. Skalak,S. Usami,S. Chien
Licensed Content Date	Jan 1, 1980
Licensed Content Volume	19
Licensed Content Issue	1
Licensed Content Pages	27
Type of Use	reuse in a thesis/dissertation
Portion	figures/tables/illustrations
Number of figures/tables/illustrations	1
Format	electronic
Are you the author of this Elsevier article?	No
Will you be translating?	No
Original figure numbers	Figure 5.
Title of your thesis/dissertation	Optimizing arteriolar network analysis using an integrated hemodynamic model derived from experimental data
Expected completion date	Aug 2018
Estimated size (number of pages)	90

Title: The microvasculature in skeletal muscle I. Arteriolar network in rat spinotrapezius muscle

Author: Erik T. Engelson,Thomas C. Skalak,Geert W. Schmid-Schönbein

Publication: Microvascular Research

Publisher: Elsevier

Date: July 1985

Order Completed

Thank you for your order.

This Agreement between Ms. Zahra Farid ("You") and Elsevier ("Elsevier") consists of your license details and the terms and conditions provided by Elsevier and Copyright Clearance Center.

Your confirmation email will contain your order number for future reference.

printable details

License Number	4417960919987
License date	Aug 28, 2018
Licensed Content Publisher	Elsevier
Licensed Content Publication	Microvascular Research
Licensed Content Title	The microvasculature in skeletal muscle I. Arteriolar network in rat spinotrapezius muscle
Licensed Content Author	Erik T. Engelson,Thomas C. Skalak,Geert W. Schmid-Schönbein
Licensed Content Date	Jul 1, 1985
Licensed Content Volume	30
Licensed Content Issue	1
Licensed Content Pages	16
Type of Use	reuse in a thesis/dissertation
Portion	figures/tables/illustrations
Number of figures/tables/illustrations	1
Format	electronic
Are you the author of this Elsevier article?	No
Will you be translating?	No
Original figure numbers	Figure 1.
Title of your thesis/dissertation	Optimizing arteriolar network analysis using an integrated hemodynamic model derived from experimental data
Expected completion date	Aug 2018

Title: Analysis of vascular pattern and dimensions in arteriolar networks of the retractor muscle in young hamsters

Author: M.L. Ellsworth,A. Liu,B. Dawant,A.S. Popel,R.N. Pittman

Publication: Microvascular Research

Publisher: Elsevier

Date: September 1987

Order Completed

Thank you for your order.

This Agreement between Ms. Zahra Farid ("You") and Elsevier ("Elsevier") consists of your license details and the terms and conditions provided by Elsevier and Copyright Clearance Center.

Your confirmation email will contain your order number for future reference.

printable details

License Number	4417961277563
License date	Aug 28, 2018
Licensed Content Publisher	Elsevier
Licensed Content Publication	Microvascular Research
Licensed Content Title	Analysis of vascular pattern and dimensions in arteriolar networks of the retractor muscle in young hamsters
Licensed Content Author	M.L. Ellsworth,A. Liu,B. Dawant,A.S. Popel,R.N. Pittman
Licensed Content Date	Sep 1, 1987
Licensed Content Volume	34
Licensed Content Issue	2
Licensed Content Pages	16
Type of Use	reuse in a thesis/dissertation
Portion	figures/tables/illustrations
Number of figures/tables/illustrations	1
Format	electronic
Are you the author of this Elsevier article?	No
Will you be translating?	No
Original figure numbers	Figure 2.
Title of your thesis/dissertation	Optimizing arteriolar network analysis using an integrated hemodynamic model derived from experimental data

RightsLink®

Home | Account Info | Help

SPRINGER NATURE

Title: Modeling study on the distribution of flow and volume in the microcirculation of cat mesentery

Author: J. S. Lee, S. Nellis

Publication: Annals of Biomedical Engineering

Publisher: Springer Nature

Date: Jan 1, 1974

Logged in as:
Zahra Farid
Account #:
3001327403

LOGOUT

Order Completed

Thank you for your order.

This Agreement between Ms. Zahra Farid ("You") and Springer Nature ("Springer Nature") consists of your license details and the terms and conditions provided by Springer Nature and Copyright Clearance Center.

Your confirmation email will contain your order number for future reference.

printable details

License Number	4417970041812
License date	Aug 28, 2018
Licensed Content Publisher	Springer Nature
Licensed Content Publication	Annals of Biomedical Engineering
Licensed Content Title	Modeling study on the distribution of flow and volume in the microcirculation of cat mesentery
Licensed Content Author	J. S. Lee, S. Nellis
Licensed Content Date	Jan 1, 1974
Licensed Content Volume	2
Licensed Content Issue	2
Type of Use	Thesis/Dissertation
Requestor type	academic/university or research institute
Format	electronic
Portion	figures/tables/illustrations
Number of figures/tables/illustrations	1
Will you be translating?	no
Circulation/distribution	<501
Author of this Springer Nature content	no
Title	Optimizing arteriolar network analysis using an integrated hemodynamic model derived from experimental data

Title: A Simple "Streak Length Method" for Quantifying and Characterizing Red Blood Cell Velocity Profiles and Blood Flow in Rat Skeletal Muscle Arterioles

Author: BARAA K. AL-KHAZRAJI, NICOLE M. NOVIELLI, DANIEL GOLDMAN, et al

Publication: Microcirculation

Publisher: John Wiley and Sons

Date: Apr 24, 2012

Order Completed

Thank you for your order.

This Agreement between Ms. Zahra Farid ("You") and John Wiley and Sons ("John Wiley and Sons") consists of your license details and the terms and conditions provided by John Wiley and Sons and Copyright Clearance Center.

Your confirmation email will contain your order number for future reference.

printable details

License Number	4417970500171
License date	Aug 28, 2018
Licensed Content Publisher	John Wiley and Sons
Licensed Content Publication	Microcirculation
Licensed Content Title	A Simple "Streak Length Method" for Quantifying and Characterizing Red Blood Cell Velocity Profiles and Blood Flow in Rat Skeletal Muscle Arterioles
Licensed Content Author	BARAA K. AL-KHAZRAJI, NICOLE M. NOVIELLI, DANIEL GOLDMAN, et al
Licensed Content Date	Apr 24, 2012
Licensed Content Volume	19
Licensed Content Issue	4
Licensed Content Pages	9
Type of use	Dissertation/Thesis
Requestor type	University/Academic
Format	Electronic
Portion	Figure/table
Number of figures/tables	1
Original Wiley	Figure 1 & Figure 4.

Title: A Microvascular Wall Shear Rate Function Derived From In Vivo Hemodynamic and Geometric Parameters in Continuously Branching Arterioles

Author: Baraa K. Al-Khazraji, Dwayne N. Jackson, Daniel Goldman

Publication: Microcirculation

Publisher: John Wiley and Sons

Date: May 6, 2016

Order Completed

Thank you for your order.

This Agreement between Ms. Zahra Farid ("You") and John Wiley and Sons ("John Wiley and Sons") consists of your license details and the terms and conditions provided by John Wiley and Sons and Copyright Clearance Center.

Your confirmation email will contain your order number for future reference.

printable details

License Number	4417970732805
License date	Aug 28, 2018
Licensed Content Publisher	John Wiley and Sons
Licensed Content Publication	Microcirculation
Licensed Content Title	A Microvascular Wall Shear Rate Function Derived From In Vivo Hemodynamic and Geometric Parameters in Continuously Branching Arterioles
Licensed Content Author	Baraa K. Al-Khazraji, Dwayne N. Jackson, Daniel Goldman
Licensed Content Date	May 6, 2016
Licensed Content Volume	23
Licensed Content Issue	4
Licensed Content Pages	9
Type of use	Dissertation/Thesis
Requestor type	University/Academic
Format	Electronic
Portion	Figure/table
Number of figures/tables	3
Original Wiley figure/table number(s)	Figure 1, Figure 7, & Figure 8.

Title: Comprehensive In Situ Analysis of Arteriolar Network Geometry and Topology in Rat Gluteus Maximus Muscle

Author: Mohammed Al Tarhuni, Daniel Goldman, Dwayne N. Jackson

Publication: Microcirculation

Publisher: John Wiley and Sons

Date: Aug 12, 2016

Order Completed

Thank you for your order.

This Agreement between Ms. Zahra Farid ("You") and John Wiley and Sons ("John Wiley and Sons") consists of your license details and the terms and conditions provided by John Wiley and Sons and Copyright Clearance Center.

Your confirmation email will contain your order number for future reference.

printable details

License Number	4417461416411
License date	Aug 28, 2018
Licensed Content Publisher	John Wiley and Sons
Licensed Content Publication	Microcirculation
Licensed Content Title	Comprehensive In Situ Analysis of Arteriolar Network Geometry and Topology in Rat Gluteus Maximus Muscle
Licensed Content Author	Mohammed Al Tarhuni, Daniel Goldman, Dwayne N. Jackson
Licensed Content Date	Aug 12, 2016
Licensed Content Volume	23
Licensed Content Issue	6
Licensed Content Pages	12
Type of use	Dissertation/Thesis
Requestor type	University/Academic
Format	Electronic
Portion	Figure/table
Number of figures/tables	1
Original Wiley figure/table number(s)	Figure 3.
Will you be translating?	No
Title of your thesis / dissertation	Optimizing arteriolar network analysis using an integrated hemodynamic model derived from experimental data
Expected completion date	Aug 2018
Expected size (number	90

Curriculum Vitae

Name: Zahra Farid

Post-secondary Education and Degrees:
University of Western Ontario
London, Ontario, Canada
2010-2016 B.Sc. (Applied Mathematics)

The University of Western Ontario
London, Ontario, Canada
2016-2018 M.Sc. (Medical Biophysics)

Honours and Awards:
Benjamin Zweifach Student Travel Award
Microcirculatory Society
2017

Publications

Refereed Articles:

Farid Z, Saleem AH, Al-Khazraji B, Jackson DN, and Goldman D. Estimating blood flow in skeletal muscle arteriolar trees reconstructed from in vivo data using the Fry approach. Microcirculation **24**: e12378.

Refereed Conference Abstracts:

Farid Z, Lemaster K, Al Tarhuni M, Frisbee JC, Jackson DN, & Goldman D. (2017). Comprehensive geometric and hemodynamic analysis of complete microvascular networks in rat gluteus maximus muscle: An integrated model derived from experimental data. *The FASEB Journal*, 31 (1 Supplement), 831-4.

Farid Z, Lemaster K, Al Tarhuni M, Frisbee JC, Jackson DN, & Goldman D. (2018). It does not do to dwell on single components and forget the importance of complete networks: Optimizing an integrated hemodynamic model derived from experimental data. *The FASEB Journal*.